AD-A 955 968

DOCUMENT SERVICE CENTER

ARMED SERVICES TECHNICAL INFORMATION AGENCY

U. B. BUILDING, DAYTON, 2, OHIO

REEL-C **5917**

A.T.I **136454**

"NOTICE: When Government or other drawings, specifications or other data are used for any purpose other than in connection with a definitely related Government procurement operation, the U.S. Government thereby incurs no responsibility, nor any obligation whatsoever; and the fact that the Government may have formulated, furnished. or in any way supplied the said drawings, specifications or other data is not to be regarded by implication or otherwise as in any manner licensing the holder or any other person or corpora- tion, or conveying any rights or permission to manufacture, use or sell any patented invention that may in any way be related thereto."

UNCLASSIFIED

ATI 136 454

WADC, RESEARCH DIV., WRIGHT-PATTERSON AIR FORCE BASE,
DAYTON, O. (AF TECHNICAL REPORT NO. 6590)

LANDING-GEAR VIBRATION - AND APPENDIXES A THRU C

MORELAND, WILLIAM J. OCT'51 76PP PHOTOS, DIAGRS, GRAPHS

AIRPLANES - VIBRATION   AIRCRAFT STRUCTURES (7)
LANDING GEARS, RETRACTABLE AEROELASTICITY (8)
WHEELS - SHIMMY
WHEELS, NOSE   UNCLASSIFIED

AF TECHNICAL REPORT NO. 6590

LANDING-GEAR VIBRATION

WILLIAM J. MORELAND
FLIGHT RESEARCH LABORATORY

OCTOBER 1951

WRIGHT AIR DEVELOPMENT CENTER

LANDING-GEAR VIBRATION

William J. Moreland
Flight Research Laboratory

October 1951

RDO No. 461-1-15

Wright Air Development Center
Air Research and Development Command
United States Air Force
Wright-Patterson Air Force Base, Dayton, Ohio

FOREWORD

This report was prepared at the Flight Research Laboratory, Wright
Air Development Center, by W. J. Moreland project engineer on RDO
Number 461-1-15, "Landing Gear Vibration." The request for this pro-
ject was initiated by Mr. Frank Minch and Dr. O. R. Rogers of the
Aircraft Laboratory. The arrangements of the equations for computation
were carried out by Paul E. Gies and George H. Moore of the Flight
Research Laboratory, Wright Air Development Center, Dayton, Ohio.
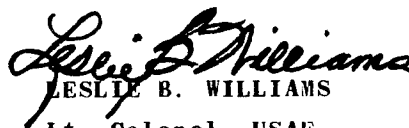
AFTR 6590

ABSTRACT

The self-excited vibration of a landing gear is generated in an interplay of effects present in the tire, the landing gear proper, and in the entire airframe itself. The analysis of these simultaneous actions is given in simple form; the manner in which energy enters the system, and the necessary structural modifications to control shimmy are explained.

PUBLICATION REVIEW

Manuscript copy of this report has been reviewed and found satisfactory for publication.

FOR THE COMMANDING GENERAL:

LESLIE B. WILLIAMS
Lt. Colonel, USAF
Chief, Flight Research Laboratory
Research Division

AFTR 6590   iii

TABLE OF CONTENTS

LIST OF ILLUSTRATIONS

<u>QUANTITY</u> <u>UNITS</u>

A	Amplitude of pivot displacement	in
a	Horizontal distance between P_1 and C.G.	in
C_c	Reference damping coefficient $(2\sqrt{K_t I_w}\,)$	in-lb-sec
C_t	Torsional damping coefficient	in-lb-sec
D	Differential operator notation	
F_l	Lateral force on swiveling structure at P_2	lbs
F_n	Ground force acting normal to wheel at P_1	lbs
F_p	Force at P_2 parallel to flight path	lbs
f	a/L	
I_g	Moment of inertia of swiveling structure about center of gravity	in-lb-sec^2
I_w	Diametral moment of inertia of the wheel	in-lb-sec^2
K_1, K_2	Lumped airframe and nose gear elasticities	lbs/in
K_v	Virtual spring constant of non-swiveling structure	lbs/in
K_t	Torsional spring constant of nose gear	in-lbs/radian
L	Trail of wheel axis behind axis of rotation of swivel	in
M	Mass of airplane	lb-sec^2/in
M_1, M_2	Lumped airframe masses	lb-sec^2/in
M_r	$(1 - f)m/N$	
m	Mass of swiveling structure	lb-sec^2/in
m_1	Mass of non-swiveling structure	lb-sec^2/in
m_s	Mass of spindle	lb-sec^2/in
m_w	Mass of wheel	lb-sec^2/in
N	$(m_1 + fm)$	lb-sec^2/in

p	Tire compressibility	in/lb
Q	$C_c V/K_t L$ (Velocity ratio)	
R	Ratio of C_t to C_c (Damping ratio)	
r_1, r_2, r_{21}	Dimensionless frequencies	
S	$4 K_t N L^2 / C_c^2$ (Mass ratio)	
s	Displacement along flight path per cycle	in
T	$L \sqrt{K_1/K_t}$ (Trail Ratio)	
T^2/S	$K_1 I_w / N K_t$ (Inertia ratio)	
U	$p K_1$	
V	Forward velocity of airplane	in/sec
W	$K_1 C V / 40 \sqrt{K_1/N}$	
x	Displacement of P_2 from equilibrium position	in
x_g	Displacement of C.G. from equilibrium position	in
Y	Displacement of wheel	in
θ	Angle made by wheel with flight path	$radians$
θ_1	Angular displacement of damper piston from its normal position	$radians$
τ	Period of vibration	$sec/cycle$
ω	Circular frequency	$radians/sec$

I. INTRODUCTION

Self-excited vibration in a landing gear nose wheel takes place because a component of the contact force between the wheel and the ground causes a drag against the forward motion of the aircraft. The energy transferred to the nose gear by this single force results in the violent motion called shimmy. If a precise mathematical description of this simple phenomenon were attempted it would involve so many parameters that solution of the problem and interpretation of the results become impractical, if not impossible. For example, in the nose gear proper, the stability of the system is influenced by the wheel load, spin-up and aerodynamic forces, gyroscopic and tire properties and, most important, nonlinearities and airframe modes of motion. However, the difficulties in the way of solution are due to the mere number of factors, and, if it can be established that some of these are more significant than others, the problem can be simplified. In this study it has been shown that the main characteristics of shimmy are dependent on the relationship of a single non-dimensional number called the "inertia ratio" and the airframe dynamics. Also, the theory developed here accounts for instability at zero trail (Schlippe reports instability at zero trail is caused by tire effects only), and the fall and rise of stability as the trail increases. The dependence of stability on mass distribution (NACA TN 760), and of frequency and damping on velocity (R.A.E.- A.D. 7/5166/G. Temple) is brought out. Guruewicz and Kruse (ATI-23097, translation) comment on the "unaccountable presence of superimposed oscillations." This effect is predicted by the theory that follows.

The landing gear of an aircraft is at best an awkward mechanical

structure. The designer is beset with a number of conflicting require-
ments and functions to perform. The gear must be able to withstand
static and dynamic loading; it must have directional stability and
permit maneuvering; it must be vertically flexible and retractable;
it must be light and of minimum overall dimensions; and it must meet
all of these requirements in extremes of enviornmental conditions.
The final design must of necessity be a compromise, and any solution
which optimises one function is not likely to be satisfactory. It is
probable, however, that much more can be achieved toward the goal
of a dynamically stable system without precision artifical damping
if close attention is given to the influence of the various physical
parameters.

In order to simplify the development of the analysis, systems of
two, three and four degrees of freedom are examined in that order.
If the effect of tire elasticity is included there is little to be
gained since the results cannot be expressed with sufficient clarity
to be useful in design. It is, however, significant to compare the
behavior of the system with and without tire elasticity by means of
an analog computer. In all the cases tested it was shown that when
the simple system was stable the higher order system was not less
stable. This problem is discussed in more detail in Appendix (B).
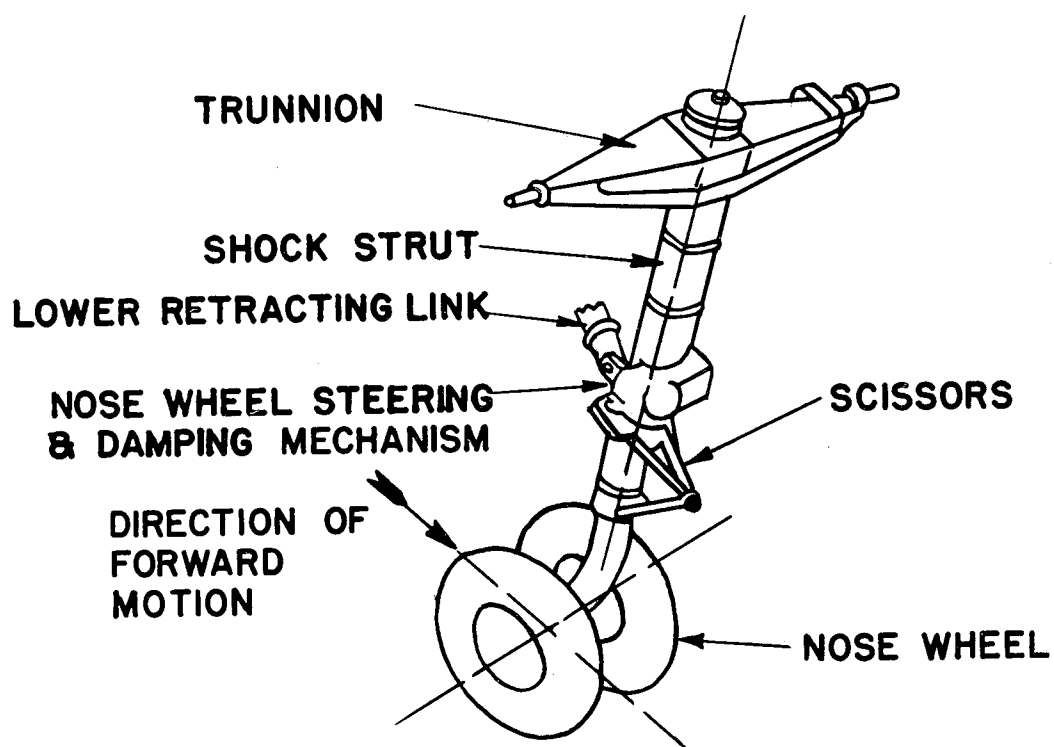

II. THE THIRD ORDER SYSTEM

The purpose of analyzing this idealized system is to explain:

a. That instability may exist for a system in which the ground
forces enter inelastically.

b. The manner in which energy is transferred from the forward
motion of the aircraft to the oscillatory motion of shimmy.

Description of the System:

The basic components of the nose wheel assembly are shown in Fig. 1 and in the schematic diagram Fig. 2. The assumption is made that the system consists of two parts - the swiveling structure of mass m which is in contact with the ground through the wheel at P_1, and the non-swiveling structure of mass m_1 which is made up of all parts not subject to the angular motion θ. These two parts are in contact at the oleo bearing P_2.

TRUNNION

SHOCK STRUT

LOWER RETRACTING LINK

NOSE WHEEL STEERING & DAMPING MECHANISM

SCISSORS

DIRECTION OF FORWARD MOTION

NOSE WHEEL

NOSE WHEEL ASSEMBLY

FIGURE 1
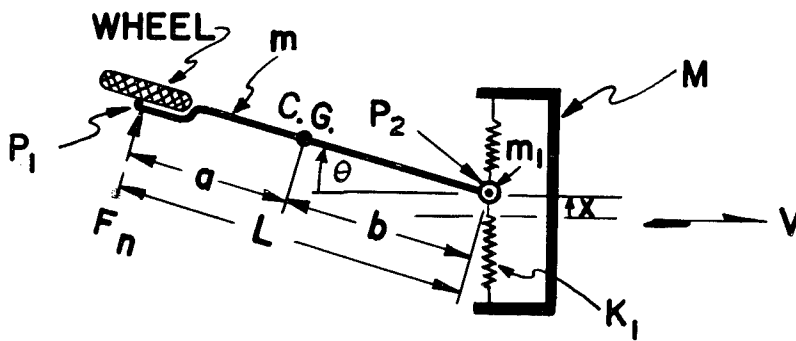
SCHEMATIC OF NOSE WHEEL ASSEMBLY
FOR THIRD ORDER SYSTEM

FIGURE 2

The following assumptions are made in the analysis:

    a. The non-swiveling structure (including the adjacent fuselage) is joined to a fixed support. The elastic restoring force on this mass m_1 due to the combined bending and twisting of the fuselage is taken proportional to x, with K_1 the equivalent elasticity.

    b. The wheel has neither side-slip nor distortion.

    c. The swiveling member is rigid.

Kinematics of the Motion:

The component velocities of P_1 and P_2, along the line joining them are equal and since P_1 has no normal velocity, the angular velocity of L can be found from the normal velocity of P_2. In Fig. 3, the velocity of the point P_2 relative to P_1 is $-L\theta$. But since P_1 has no velocity normal to the link L, the normal velocity of P_2 is also
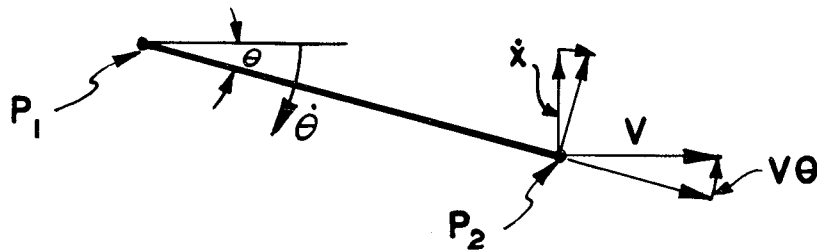
KINEMATICS OF SWIVELING MEMBER

FIGURE 3

the relative velocity of P_2 to P_1. Hence for small values of θ,

$$-L\dot{\theta} = \dot{x} + V\theta$$

$$-\dot{\theta} = \frac{\dot{x}}{L} + \frac{V\theta}{L} \qquad (1)$$

Eq. 1 shows that the two degrees of freedom are kinematically coupled. Eq. 1 can be developed to show the nature of the motion of the system.

From Fig. 4, let

$$Y = x + L\theta$$

$$\therefore \theta = \frac{Y - x}{L}$$

$$\dot{\theta} = \frac{\dot{Y} - \dot{x}}{L}$$

Substitute in (1)

$$-\dot{Y} + \dot{x} = \dot{x} + \frac{V}{L}(Y - x)$$
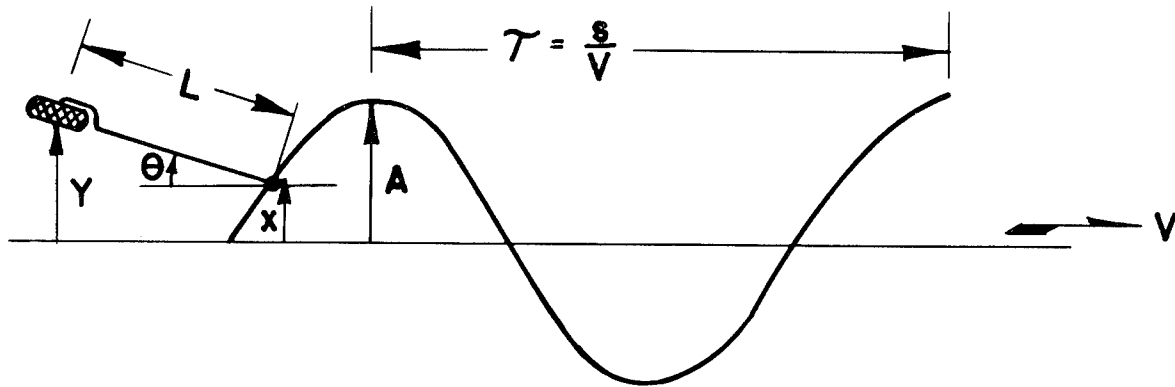
GEOMETRY OF THE MOTION OF THE SWIVELING MEMBER.
FIGURE 4

$$-\dot{Y} = \frac{V}{L}(Y - x) = V\theta \tag{1A}$$

If the motion of P_2 is assumed sinusoidal and of amplitude A, then

$$\dot{Y} + \frac{V}{L}Y = \frac{V}{L}x = (\frac{V}{L}A)\ sin\ \omega t$$

$$\therefore Y = \frac{\frac{V}{L}A\ sin\left[\omega t - tan^{-1}\frac{\omega}{(\frac{V}{L} - 0)}\right]}{\sqrt{(\frac{V}{L} - 0)^2 + \omega^2}} \tag{2}$$

The amplitude of Y may be expressed independent of frequency. Thus

$$\tau = \frac{s}{V} \qquad\qquad or \qquad\qquad V = \frac{s}{\tau} = \frac{s}{2\pi/\omega}$$

Hence

$$Y = \frac{\frac{V}{L} A \sin\left[\frac{2\pi}{s} Vt - \tan^{-1}\frac{2\pi V}{sV/L}\right]}{\sqrt{\left(\frac{V}{L}\right)^2 + \frac{4\pi^2 V^2}{s^2}}}$$

or,

$$Y = \frac{A}{\sqrt{1 + \left(\frac{L}{s}\right)^2 4\pi^2}} \sin\left[(2\pi/s)Vt - \tan^{-1} 2\pi L/s\right] \qquad (3)$$

The amplitude of P_1 is always less than A and lags behind the spindle position by an angle less than 90 degrees. For example, when $(L/s) << 1/4\pi^2$, the amplitude of the motion of P_1 approaches that of P_2. Also,

$$tan\ lag \to 0 \quad and\ lag \to 0$$

And for $(L/s) >> 1/4\pi^2$, the amplitude of the motion of P_1 approaches zero, while the lag angle approaches 90 degrees.

Dynamics of the Motion:

The following factors have been neglected in the analysis:

a. Backlash.

b. Coulomb friction.

c. Moment caused by the weight on the nose-wheel acting through the moment arm due to the laterally deflected nose-wheel.

d. Elasticity of the tire.

e. Gyroscopic effects. Preliminary analysis indicates that gyroscopic effects will alter principally the magnitude rather than the nature of the motion. Moreover, it appears that local elastic effects will considerably reduce the gyroscopic torques.

The force at P_1 (Fig. 2) between the wheel and the ground is F_n normal to the plane of the wheel. The elastic restoring force $K_1 x$ acts on m_1 but the force that reaches the swiveling structure at P_2 is $K_1 x + m_1 \ddot{x}$. (i.e. the greater $\ddot{x}$ becomes, the greater will be the reaction on the pivot P_2. This is in the same direction as the spring reaction. Hence, $Force = K_1 x + m_1 \ddot{x}$). Then the force equation becomes (for small values of θ).

$$F_n - (K_1 x + m_1 \ddot{x}) = m \ddot{x}_g = m(\ddot{x} + b \ddot{\theta}) \qquad (4)$$

and for the moments about the $C.G.$, for small values of θ,

$$F_n a + (K_1 x + m_1 \ddot{x})b - C_t \dot{\theta} = I_g \ddot{\theta} \qquad (5)$$

By eliminating F_n in (4) and (5)

$$(K_1 x + m_1 \ddot{x})a + (\ddot{x} + b \ddot{\theta})am + (K_1 x + m_1 \ddot{x})b - C_t \dot{\theta} = I_g \ddot{\theta} \qquad (6)$$

Eq. 1 can be rewritten,

$$\dot{x} = -L \dot{\theta} - V \theta$$

Successive differentiation of this form and substitution in (6) gives

$$(I_g + ma^2 + m_1L^2)\,\dddot{\theta} + (C_t + amV + m_1LV)\,\ddot{\theta} + K_1L^2\,\dot{\theta} + K_1LV\,\theta = 0 \qquad (7)$$

or

$$\dddot{\theta} + \frac{(C_t + amV + m_1LV)}{(I_g + ma^2 + m_1L^2)}\,\ddot{\theta} + \frac{K_1L^2}{(I_g + ma^2 + m_1L^2)}\,\dot{\theta} + \frac{K_1LV}{(I_g + ma^2 + m_1L^2)}\,\theta = 0 \qquad (8)$$

Applying Routh's criterion for stability,

$$\left(\frac{C_t + amV + m_1LV}{I_g + ma^2 + m_1L^2}\right)\left(\frac{K_1L^2}{I_g + ma^2 + m_1L^2}\right) > \left(\frac{K_1LV}{I_g + ma^2 + m_1L^2}\right)$$

$$C_tL + amVL + m_1VL^2 > I_gV + ma^2V + m_1VL^2$$

$$C_t > \frac{V}{L}\left[I_g + ma^2 - (ma^2 + mab)\right]$$

$$C_t > \frac{V}{L}(I_g - mab) \qquad (9)$$

Considering usual proportions of nose-wheel assemblies, most of the swiveling structure can be considered as concentrated at the wheel and at the spindle P_2. Then

$$a = L\,\frac{m_s}{m} \; ; \quad b = L\,\frac{m_w}{m}$$

and considering the moment of inertia of the spindle about its own axis negligible in comparison with I_w ,

$$I_g = I_w + m_wa^2 + m_sb^2 = I_w + L^2\,\frac{m_sm_w}{m} \qquad (10)$$

Combining (9) and (10)

$$C_t > \frac{V}{L}\left[I_w + m\left(\frac{Lm_s}{m}\right)\left(\frac{Lm_w}{m}\right) - mab\right]$$

or,

$$C_t > \frac{V}{L}(\dot{I}_w) \qquad\qquad (11)$$

It follows from Eq. 11 that for the structural proportions found in practice, the system (idealized as in Fig. 2) is inherently unstable. The damping required for stability increases with velocity and moment of inertia of wheel and decreases with increasing trail. It will be of some interest to examine how these conclusions may be altered, even qualitatively, for apparently minor changes in the physical system.

Energy Analysis:

In order to obtain a clear picture of the manner in which energy is transferred from the forward motion of the aircraft to the swiveling structure, the following energy analysis is useful:
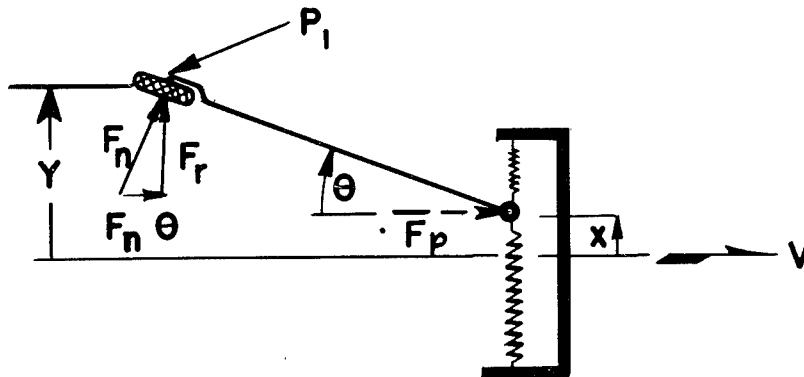
ENERGY ANALYSIS DIAGRAM

FIGURE 5

Assume: (a) No slipping at P_1.

(b) The velocity of the aircraft remains constant in magnitude and direction.

(c) The mass of the swiveling structure is concentrated at P_1.

(d) The mass m_1 equal to zero.

From Fig. 5:

Forces:

$$F_n - K_1 x = m_w \ddot{Y} \tag{12}$$

$$F_n \theta + F_p = m_w (L\ddot{\theta} \times \theta + L\dot{\theta}^2) \tag{13}$$

Torques:

$$K_1 x L - F_p L\theta - C_t \dot{\theta} = I_w \ddot{\theta} \tag{14}$$

From (12) and (13):

$$F_p = -(K_1 x + m_w \ddot{Y})\,\theta + m_w (L\ddot{\theta} \times \theta + L\dot{\theta}^2) \tag{15}$$

The work required to maintain the velocity of the aircraft is:

Work done against $F_p = \int_0^\tau F_p V\,dt$ **for one cycle.**

Hence from (15):

$$W_p = -V \int_0^\tau (K_1 x + m_w \ddot{Y})\,\theta\,dt + m_w V \int_0^\tau L(\ddot{\theta} \times \theta + \dot{\theta}^2)\,dt \tag{16}$$

If x is assumed to vary harmonically, then

$$x = A\ \sin \omega t \tag{17}$$

and

$$Y = \frac{A}{H}\ \sin\ (\omega t - \varphi)$$

Where from *(3),*

$$H = \sqrt{1 + \left(\frac{L}{s}\right)^2 4\pi^2} \qquad \text{and} \qquad \varphi = \tan^{-1}\frac{\omega L}{V}$$

$$\therefore \ddot{Y} = -\frac{A\omega^2}{H} \sin(\omega t - \varphi) \qquad\qquad (18)$$

$$\theta = -\frac{\dot{Y}}{V} = -\frac{\omega A}{HV} \cos(\omega t - \varphi) \qquad \text{(See Eq. 1A)} \qquad (19)$$

From *(16),*

$$\int_0^\tau \dot{Y}\theta \, dt = \frac{\omega^3 A^2}{H^2 V} \int_0^{2\pi} \sin(\omega t - \varphi) \cos(\omega t - \varphi) \frac{d(\omega t)}{\omega} = 0$$

Hence *(16)* **becomes:**

$$W_p = -VK_1 \int_0^\tau x\theta \, dt + m_w V \int_0^\tau L(\ddot{\theta} \times \theta + \dot{\theta}^2) \, dt$$

Since the second integral is zero for the complete cycle, it follows from *(17)* and *(19)*

$$W_p = +\frac{K_1 V A^2}{HV} \omega \int_0^\tau \sin\omega t \, [\cos(\omega t - \varphi)] \, dt$$

$$W_p = \frac{K_1 A^2}{H} \omega \sin\varphi \int_0^{2\pi} \sin^2\omega t \frac{d(\omega t)}{\omega}$$

$$W_p = K_1 \frac{A^2}{H} \pi \sin\varphi \qquad\qquad (20)$$

(Tire elasticity will increase the lag angle φ).

Energy Analysis Discussion.

Eq. 20 shows that energy can be transferred from the forward

motion of the aircraft to the oscillatory motion of shimmy only if a phase lag φ exists. Eq. 3 shows that for the system under discussion a finite phase lag between $0°$ and $90°$ will always be present. An examination of Fig. 5 and the above analysis will make it clear that the force being overcome in the forward motion is the parallel component of the ground force ($F_n\theta$) at the wheel. And because of the phase lag φ, this force is directed predominantly __against__ the motion of the aircraft. Moreover, this same force in combination with the elastic force at the spindle produce the uncompensated angular acceleration which stores energy in the swiveling structure which is the observed shimmy. In the event that the precise amount of damping, $C_t = (V/L)I_w$, required to prevent instability is supplied, then the steady state motion will be truly harmonic and all the energy supplied will be absorbed by the damper. The proof may be obtained from Eq. 14 as follows:

The energy absorbed by the damper is,

$$E = \int C_t \dot{\theta} \, d\theta \quad \text{over one cycle of } \theta$$

Mult. *(14)* by $d\theta$

$$C_t \dot{\theta} \, d\theta = (K_1 xL - F_p L\theta) \, d\theta - I_w \ddot{\theta} \, d\theta = dE$$

Since $\int I_w \ddot{\theta} \, d\theta = 0$ for one cycle of sinusoidal motion,

$$E = \int (K_1 xL - F_p L\theta) \, d\theta \tag{21}$$

But, $-\int F_p L\theta \, d\theta = L\int (K_1 x + m_w \ddot{Y}) \, \theta^2 \, d\theta$ which is negligible for small values of θ

Hence *(21)* **becomes:**

$$E = K_1 L \int x \, d\theta$$

$$E = \frac{K_1 L A^2 \omega^2}{HV} \int_0^\tau \sin \omega t \, [\sin(\omega t - \varphi)] \, dt$$

or,
$$E = \frac{K_1 L A^2 \omega^2}{HV} \cos \varphi \int_0^{2\pi} \sin^2 \omega t \, \frac{d(\omega t)}{\omega}$$

$$\therefore E = \left(\frac{K_1 A^2}{H}\pi\right)\left(\frac{L\omega}{V}\right) \cos \varphi$$

But,

$$\frac{L\omega}{V} = \tan \varphi \quad \textbf{(Eq. 3)}$$

Hence,

$$E = K_1 \frac{A^2}{H} \pi \sin \varphi \qquad (22)$$

Therefore the energy absorbed by the damper is precisely that supplied to maintain the constant velocity of the aircraft. (See Eq. 20).

III. THE FOURTH ORDER SYSTEM

With sufficient data on the distribution of mass and elasticity of the nose-wheel gear and its supporting structure, and on the nature of the external forces that enter the system, it is possible to set up differential equations that describe the system more or less accurately. Added degrees of freedom, however, increase the difficulty of interpreting the solutions, and, if the supporting data is in-

accurate, may be of no practical value at all. The following equations describe an idealized system of three degrees of freedom, which, though neglecting such factors as the decrease in lateral elasticity caused by the offset vertical load, and the load peculiar to tire elasticity which in a true shimmy may be small, reveals factors of some significance.
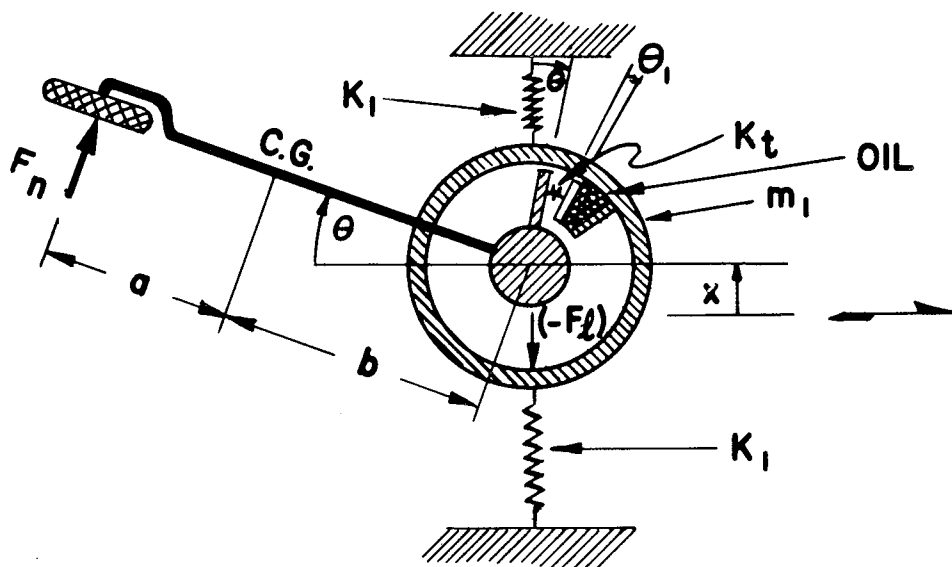
FOURTH ORDER SYSTEM

FIGURE 6

Fig. 6 is a schematic diagram of the three degrees of freedom system. An angular displacement θ of the nose-wheel is transmitted to one end of the elastic member K_t, the other end of which drives the damper piston through the displacement θ_1. The force in the elastic member due to its distortion $K_t(\theta - \theta_1)$ is the same as that

transmitted to the damper piston $C_t\dot{\theta}_1$. (It is immaterial whether the elastic member comes before or after the damper). The analysis is:

Forces:

$$F_n + F_l = m\ddot{x}_g \qquad (23)$$

$$- K_1 x - F_l = m_1 \ddot{x} \qquad (24)$$

Swivel Torque:

$$F_n a - F_l b - (damper\ torque) = I_g \ddot{\theta} \qquad (25)$$

Damper Torque:

$$C_t \dot{\theta}_1 = K_t(\theta - \theta_1) \qquad (26)$$

Kinematic:

$$- L\dot{\theta} = \dot{x} + V\theta \qquad (27)$$

Geometric:

$$x_g = x + b\theta \qquad (28)$$

The above six equations contain six variable functions of time. Eliminating F_n, F_l and θ_1 gives,

$$C_t K_t \dot{\theta} = [a(K_1 x + m_1 \ddot{x} + m\ddot{x}_g) + b(K_1 x + m_1 \ddot{x}) - I_g \ddot{\theta}](C_t + K_t/D)D \qquad (29)$$

Differentiating (29) and combining with (27) and (28) gives,

$$[C_t(I_g + m_1 L^2 + ma^2)]\ \ddddot{\theta} + [K_t(I_g + m_1 L^2 + ma^2) + C_t V(m_1 L + ma)]\ \dddot{\theta} +$$

$$[K_t V(m_1 L + ma) + C_t(K_t + K_1 L^2)]\ \ddot{\theta} + [K_1(C_t LV + K_t L^2)]\ \dot{\theta} + [K_1 K_t LV]\ \theta$$

16 $= 0 \qquad (30)$

Applying Routh's criterion for stability to this fourth order equation gives,

$$[K_t(I_g + m_1L^2 + ma^2) + C_tV(m_1L + ma)] [C_t(K_t + K_1L^2) + K_tV(m_1L + ma)] >$$

$$K_1L(K_tL + C_tV) \, C_t(I_g + m_1L^2 + ma^2)$$

$$+ \frac{K_1K_tLV \, [\, K_t(I_g + m_1L^2 + ma^2) + C_tV(m_1L + ma)]^2}{K_1K_tL^2 + C_tK_1LV} \qquad (\,31\,)$$

The inequality (31) contains nine parameters. If we elect, for example, to solve for the threshold value of C_t sufficient to establish equilibrium it is a cubic equation in C_t with eight independent parameters. Since the equation contains the three fundamental units of length, force, and time, it follows from the laws of dimensional analysis that the number of essential parameters can be reduced by three if the equation is expressed in non-dimensional form. Moreover, if the given relationship involves more than one of the same kind of quantity, such as several lengths and masses, then all of the same kind of quantity can be expressed in terms of one of them and ratios of the others to it. In this way, as shown in the appendix, the eight independent parameters of (31) are reduced to three. By this means it is possible to reveal the conditions that must be met to insure that a simultaneous change in the variables will represent an essential change in the dynamic characteristics of the system. The four non-dimensional parameters used to describe the system are:

$$R = C_t \, / \, C_c = C_t \, / \, 2\sqrt{K_tI_w}$$

$$Q = C_cV \, / \, K_tL$$

$$T = L \sqrt{K_1/K_t}$$

$$S = 4NK_t L^2/C_c^2 \qquad\qquad (\textit{Where } N = m_1 + fm)$$

In terms of these dimensionless quantities, the inequality (31) becomes:

$$QS(1 - T^2/S)\ R^3 + [1 + S(2 - T^2/S)]\ R^2 + [(1 + S)/Q - QS/4]\ R$$
$$- (1 + S)/4 = 0 \qquad (32)$$

This equation will be used in the remainder of the report to describe the influence of all the essential parameters on the dynamics of the nose gear.

The dimensionless quantity T^2/S, hereinafter referred to as the " inertia ratio " is the number which serves to identify the nature of the damping requirements for stability of any particular system. The significance of the dimensionless parameters in eq. (32) can best be exposed by plotting values of the threshold damping ratio R (i.e., R that makes the left member equal to zero) versus T^2/S, the inertia ratio. From the definitions of T and S the inertia ratio is

$$T^2/S = K_1 C_c^2/4K_t^2 N = \frac{I_w}{NK_t\ /\ K_1}$$

a quantity independent of the trail L for constant values of a/L. From Descartes' rule of signs or an inspection of Fig. 7a, it can be seen that for values of the inertia ratio less than unity the cubic in R can have no more than one positive root, and hence the system will be stable for all values of R above those values shown by the ordinates of the graph. For values of the inertia ratio above unity there is at first a range in which there are two positive roots-

and hence the system can be stable only <u>between</u> these two values of
R. Finally, beyond this range, there is a region of no positive roots
which means that the system cannot be stabilized regardless of the
damping applied. Graphs of damping ratio versus inertia ratio may be
plotted for a range of values of the dimensionless parameters Q and
S. These charts can then be entered for any given system under study
by computing the values of Q, S and T^2/S. It can then be directly
determined whether the system is stable or not and whether the damp-
ing range is limited or unlimited. In order to determine what adjust-
ments in the dynamic parameters of the system would be required so
that a satisfactory point on the stability chart would be occupied,
(32) may be examined for the inertia ratio value of unity. For this
case *(32)* becomes quadratic from which

$$R = \frac{[\frac{QS}{4(1+S)} - \frac{1}{Q}] \pm \sqrt{[\frac{QS}{4(1+S)} - \frac{1}{Q}]^2 + 1}}{2}$$

Reducing the values of Q and S will lower R which means that the point
on the chart showing the actual system damping has penetrated further
upward into the stability region. Hence, stability can be adjusted
favorably in this region by lowering T^2/S, Q and S simultaneously.
This may be accomplished, for example, by reducing the lateral elast-
icity and the mass of the system and increasing the torsional elast-
icity. It would be of some value to be able to determine the magnitude
of the inertia ratio beyond which stability is impossible. Since the
limit of stability is characterized by the cubic in R having two
equal roots (see Fig. 7a) the relationship between the parameters
may be found by setting the discriminant of *(32)* equal to zero. For

example, if the coefficients of R^3, R^2, R in *(32)* are a, b, c, respectively and the constant term is d then the solution of the following equation for T^2/S will be the value of the inertia ratio beyond which stability is impossible:

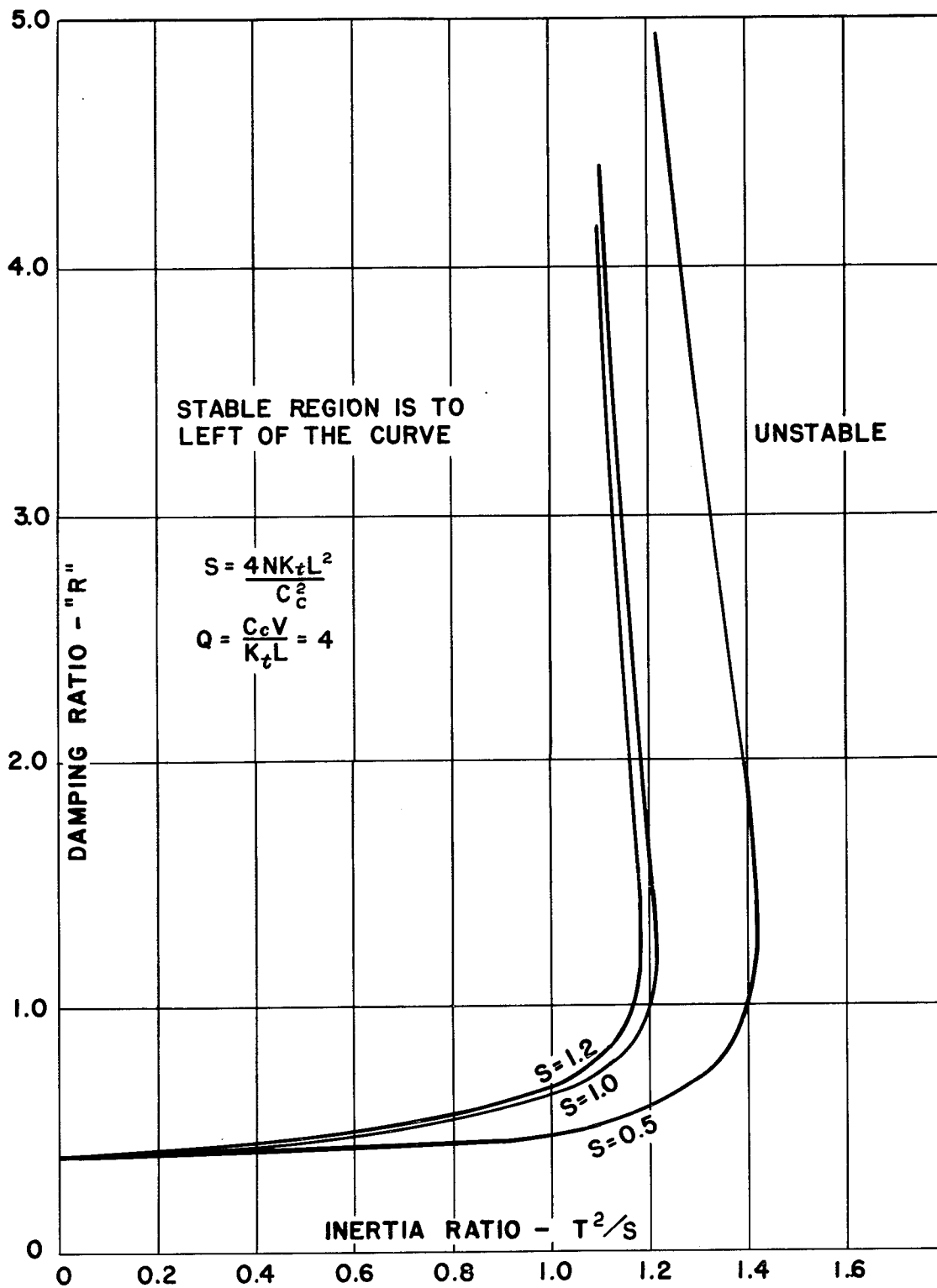$$18\ abcd - 4\ b^3 d - 4\ c^3 a + b^2 c^2 - 27\ a^2 d^2 = 0$$

If it is desired to extend the range of T^2/S it is apparent from Fig. 7a and 7b that this may be accomplished by reducing the parameters S and Q.

If Fig. 7b is plotted in three dimensions as shown in Fig 7c, a clearer picture is obtained of the region of stability. The stable region is <u>inside</u> the surface. It will be noted that, as Q becomes large, the surface approaches the plane $T^2/S = 1$. Physically, this may be caused by an increase in velocity. The maximum taxi velocity (and hence the maximum Q) will be determined from aerodynamic considerations. This value of Q can then be used to determine the value of T^2/S required for the operating point to remain in the stable region.

In the previous discussion the surface of neutral stability was considered. Another consideration is how the degree of stability changes as points move into or away from the line of neutral stability.

The investigation was accomplished by assigning values to the parameters in the fourth order equation and placing the resulting equation in θ, on an analog computer. The logarithmic decrements were then determined and plotted (Fig. 7d).

Two points of interest are to be noted. First for a given value of R, relatively large changes of the inertia ratio can be made with-

STABLE REGION IS TO
LEFT OF THE CURVE

UNSTABLE

$$S = \frac{4NK_tL^2}{C_c^2}$$

$$Q = \frac{C_cV}{K_tL} = 4$$

DAMPING RATIO – "R"

S=1.2
S=1.0
S=0.5

INERTIA RATIO – T^2/S

DAMPING RATIO FOR NEUTRAL STABILITY vs. INERTIA RATIO

FIGURE 7a

DAMPING RATIO FOR NEUTRAL STABILITY vs. INERTIA RATIO
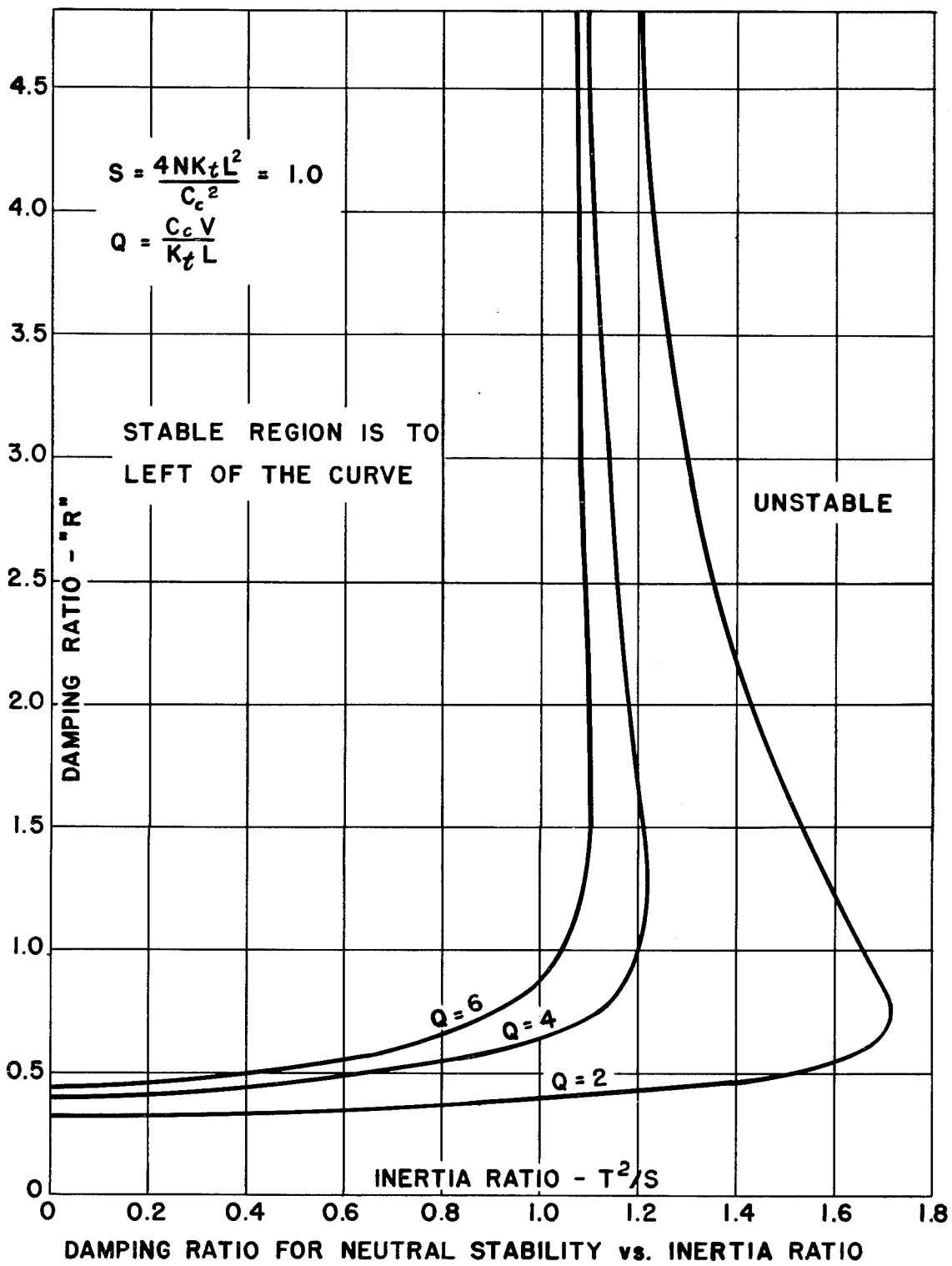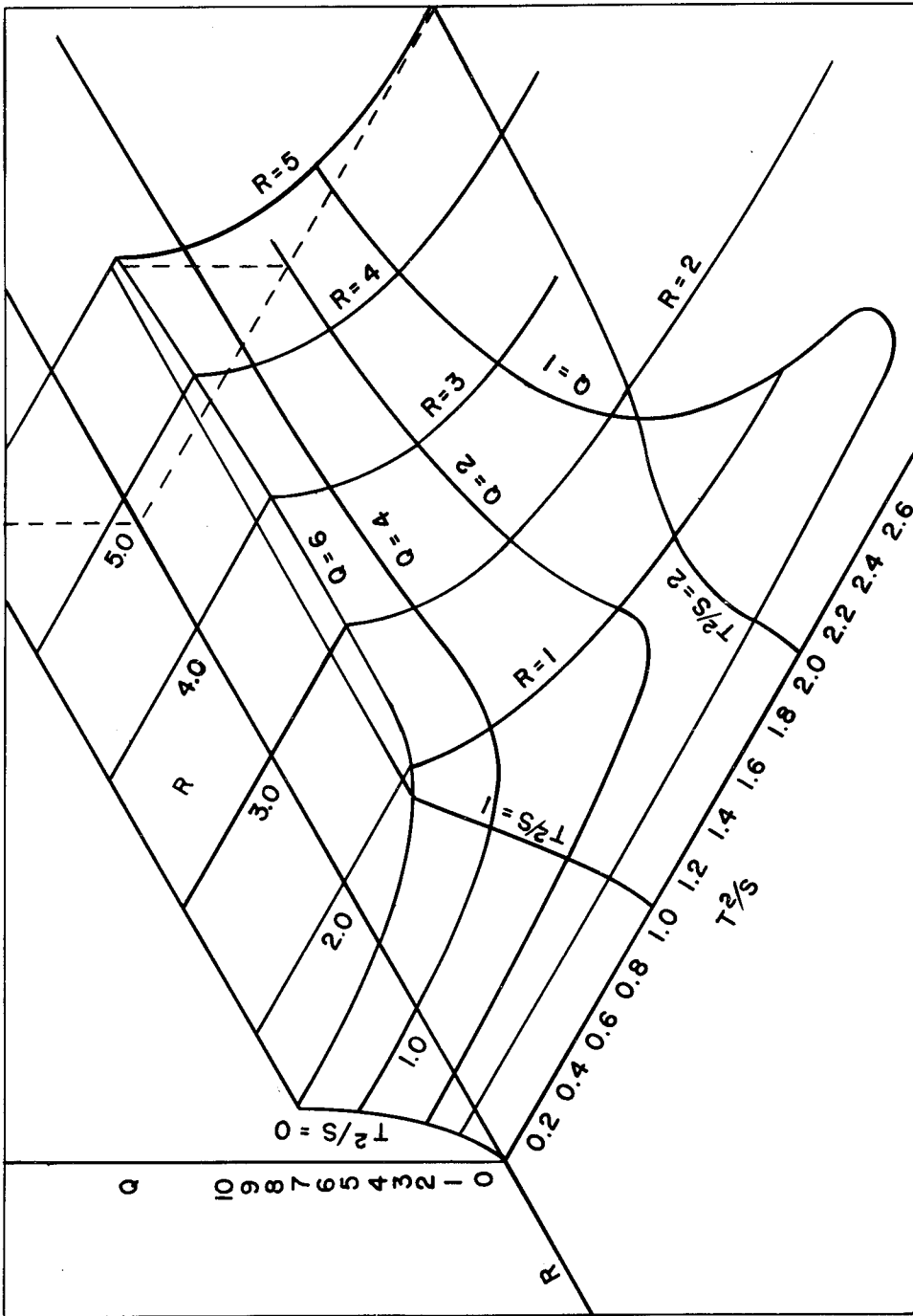
FIGURE 7 b

STABLE SURFACE   S = 1.0
STABLE REGION IS "INSIDE" THE SURFACE

STABILITY SURFACE
FIGURE 7c

CONTOURS OF EQUAL

LOGARITHMIC DECREMENT

BASED ON ANALOG STUDIES

CONSTANTS: Q=2 S=1

INERTIA RATIO = $\dfrac{I_w K_1}{K_t (m_1 + \frac{q}{L} m)}$
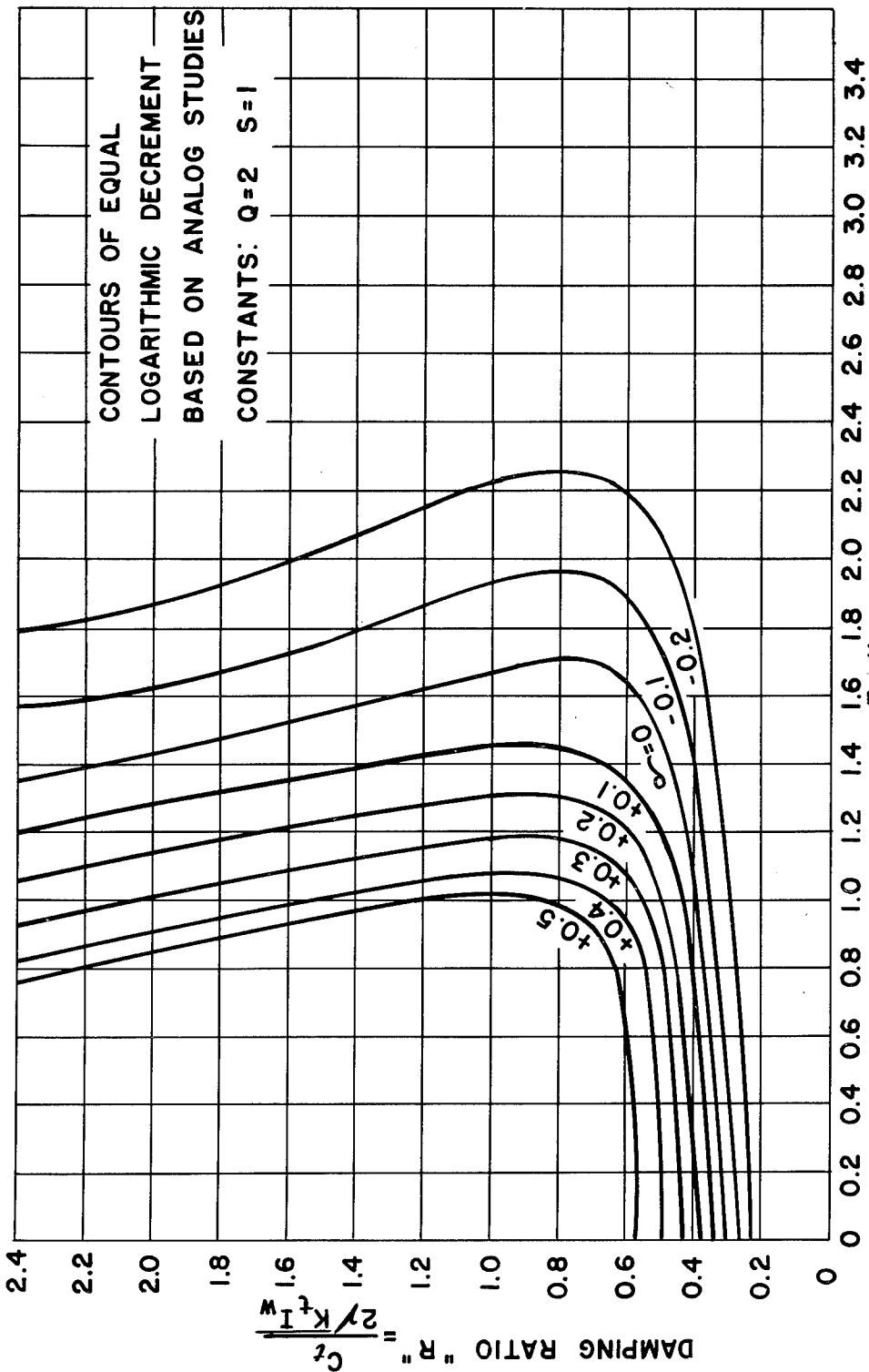
STABILITY INTENSITY DIAGRAM

FIGURE - 7d

DAMPING RATIO "R" = $\dfrac{C_t}{2\sqrt{K_t I_w}}$

-0.2

-0.1

$\searrow = 0$

+0.1

+0.2

+0.3

+0.4

+0.5

out appreciably changing the rate of growth or decay of the shimmy when operating close to the stability surface. Second, for low values of the inertia ratio the rate of growth or decay of the shimmy is changed considerably with a small change in R.

Analysis of the Requirements for Threshold Stability:

Case I. <u>Zero Damping</u>. If C_t is taken as zero, (31) becomes

$$K_t(I_g + m_1L + ma^2)K_tV(m_1L + ma) = \frac{K_1K_tLVK_t^2(I_g + m_1L^2 + ma^2)^2}{K_1K_tL^2}$$

or

$$L = a + I_g/ma$$

but

$$I_g = I_w + maL - ma^2$$

$$\therefore L = L + I_w/ma$$

Hence, with no damping the system is inherently unstable. The requirement for stability can be approached by reducing the inertia of the nose-wheel relative to the trail and mass of the system.

Case II. <u>Zero Trail</u>. As the trail L approaches zero, (31) becomes, for any finite value of the velocity V

$$[K_tI_g][C_tK_t] = \frac{K_1K_tV[K_tI_g]^2}{C_tK_1V}$$

or

$$C_t^2 = K_tI_w = C_c^2/4$$

or

$$R = 1/2$$

Hence, as the trail approaches zero, the damping ratio approaches 1/2, and the absolute damping coefficient C_t may be reduced by lowering the torsional elasticity and the inertia of the wheel.

Case III. <u>Zero Trail</u>. At zero trail determine the partial derivative of the damping ratio with respect to the trail. This quantity determines whether the required damping for a given system increases or decreases in value as the trail is increased from zero. From (32) with $L \rightarrow 0$, and $R = 1/2$

$$\frac{\partial R}{\partial L} = \frac{C_c V K_1}{8 K_t^2} - \frac{K_t}{2 C_c V}$$

Since this expression may be positive or negative it follows that increasing the trail from zero may require more or less damping depending upon the relative magnitudes of the two terms. Expressing the above relation in terms of the dimensionless parameters of the system gives

$$\frac{\partial R}{\partial L} = \frac{Q T^2}{8L} - \frac{1}{2QL}$$
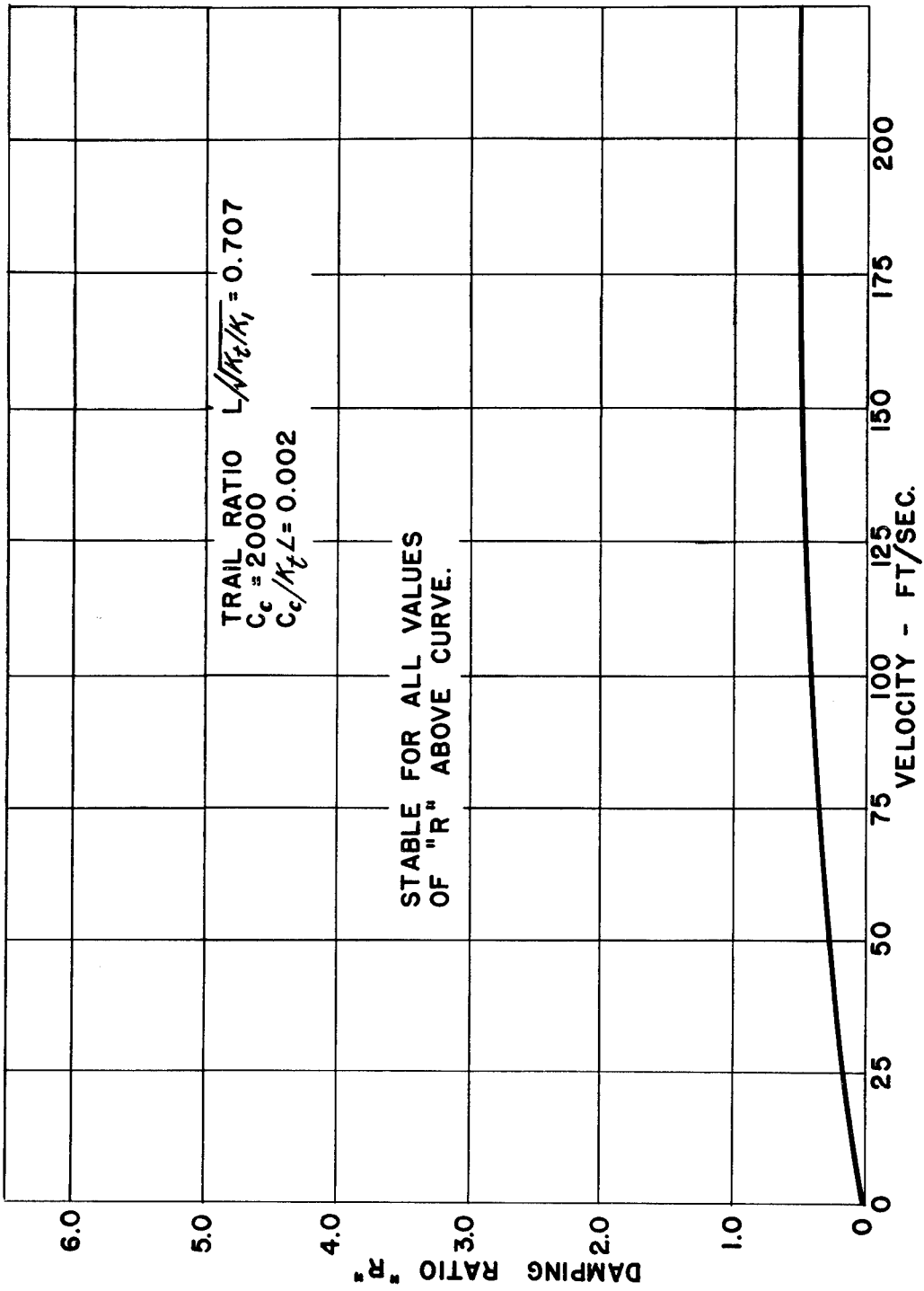
and the condition for zero slope is

$$QT = 2$$

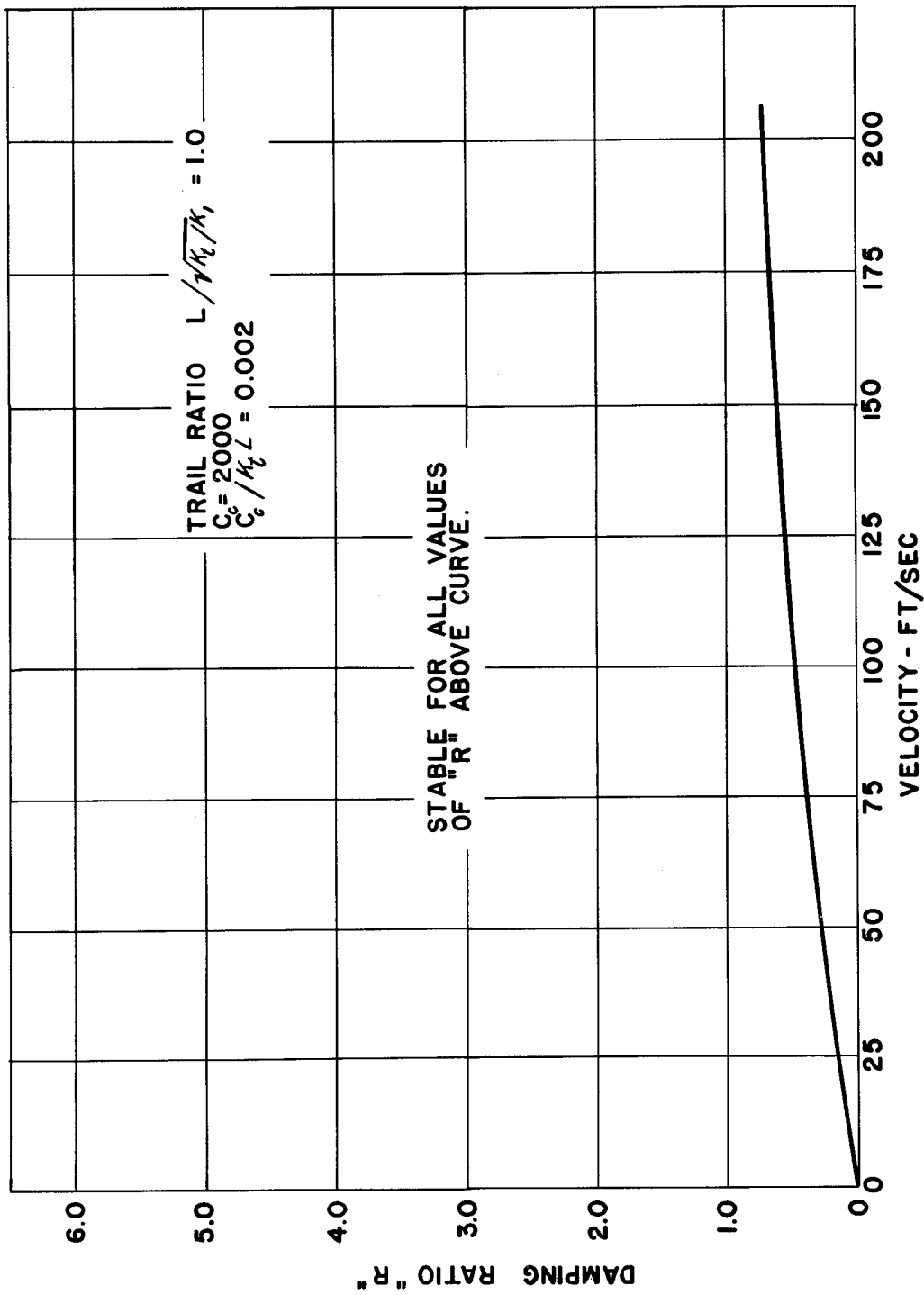If the dimensionless product QT exceeds 2, the damping ratio must

be made greater than 1/2 to maintain stability; for QT less than 2 the threshold damping ratio becomes less than 1/2 as the trail increases. (See Fig. 9a)

Case IV. <u>Effect of Velocity on Stability</u>. This relationship can be depicted by plotting R as a function of Q, since Q is proportional to V. Figs. 8a, 8b, 8c, are plotted for values of the trail ratio T of 0.707, 1.0 and 1.118 respectively. For convenience S has been taken as unity and $C_c/K_t L$ as 0.002. Inspection of these figures indicates that the damping requirement increases as the velocity increases, but for values of the "inertia ratio", T^2/S, greater than 1.0, there is an upper limit to the damping that will stabilize the system. As the velocity increases these two damping values coalesce, and above this critical velocity no stability is possible. (See Fig. 8c)

Case V. <u>Effect of Trail on Stability</u>. For this case the value of R may be plotted as a function of the trail ratio T. It is to be noted that Q and S are each functions of L and hence both of these parameters must be recalculated for each point plotted. For values of the inertia ratio less than unity, stability is possible for all values of the trail - the required damping usually increasing with trail to a maximum and thereafter approaching zero asymptotically. These results are shown in Fig. 9a. For values of the inertia ratio slightly above unity the range of damping for stability is limited (e.g. between branches of $T^2/S = 1.1$, as shown in Fig. 9b). For values of the inertia ratio above a certain critical value there are intermediate values of the trail ratio for which stability is impossible (e.g. with $T^2/S = 1.25$, the system is unstable regardless of the damping employed if the trail ratio lies between 0.55 and

DAMPING RATIO FOR NEUTRAL STABILITY vs. VELOCITY

FIGURE 8a

TRAIL RATIO $L\sqrt{K_t/K_i} = 0.707$
$C_c = 2000$
$C_c/K_t L = 0.002$

STABLE FOR ALL VALUES OF "R" ABOVE CURVE.

VELOCITY - FT/SEC.

DAMPING RATIO "R"

TRAIL RATIO $L/\sqrt{k_\zeta/k_r} = 1.0$
$C_c = 2000$
$C_c^2/k_\zeta L = 0.002$

STABLE FOR ALL VALUES
OF "R" ABOVE CURVE.

DAMPING RATIO FOR NEUTRAL STABILITY vs. VELOCITY

FIGURE 8b

VELOCITY - FT/SEC

DAMPING RATIO "R"

TRAIL RATIO $L\sqrt[4]{K_t}/K_1 = 1.118$
$C_c = 2000$
$C_c/K_t L = 0.002$

STABLE REGION

VELOCITY – FT/SEC

DAMPING RATIO FOR NEUTRAL STABILITY vs. VELOCITY

FIGURE 8c

DAMPING RATIO – "R"

$$\frac{I^2}{S} = \frac{I_w}{NK_t/K_i} = 0.833$$

CURVES SHOWING EFFECT OF
VELOCITY AND TRAIL ON
NOSE-WHEEL STABILITY

STABLE FOR ALL VALUES
OF "R" ABOVE CURVE

V=2000 "/sec

V=1500 "/sec

V=1000 "/sec

TRAIL RATIO - L $\sqrt{K_1/K_t}$

FIGURE 9a

DAMPING RATIO - "R"

0.8   0.7   0.6   0.5   0.4   0.3   0.2   0.1   0

0   1   2   3   4

CURVES SHOWING EFFECT OF
INERTIA RATIO & TRAIL ON
NOSE WHEEL STABILITY

$$\frac{I^2}{S} = \frac{I_w}{N K_t / K_l}$$

DAMPING RATIO "R"

TRAIL RATIO - $L \sqrt{K_l / K_t}$

FIGURE 9 b

and 1.9, Fig. 9b), and outside these values stability is possible but only over limited ranges of damping.

Solution of Equation (30)

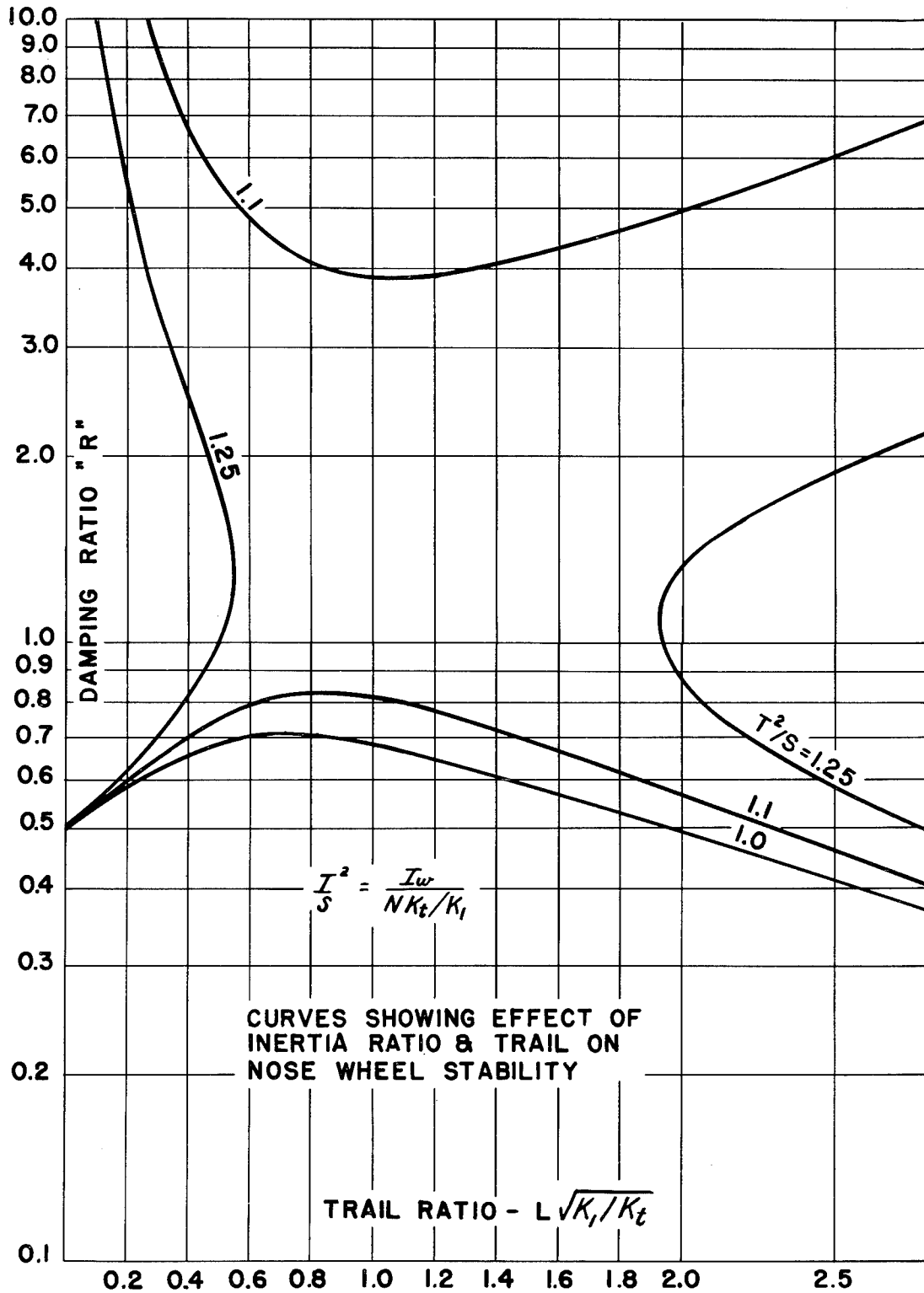Eq. 30 may be expressed in non-dimensional form as shown in Appendix A. Thus

$$D^4\theta \;+\; \frac{(\,T/2\sqrt{S}\,)\,[\;1 + S(\;1 + QR\;)\,]}{(\;1 + S\;)\,RT^2/S}D^3\theta \;+$$

$$\frac{[(\;1 + T^2\;)R + QS/4\;]}{(\;1 + S\;)RT^2/S}D^2\theta \;+\; \frac{(\,T/2\sqrt{S}\,)\,S(\;1 + QR\;)}{(\;1 + S\;)\,RT^2/S}D\theta$$

$$+\; \frac{QS/4}{(\;1 + S\;)\,RT^2/S}\theta \;=\; 0 \qquad\qquad (33)$$

where the derivative is taken with respect to the dimensionless time $\sqrt{K_1/N}\times t$. The solution of Eq. 33 is:

$$\theta \;=\; C_1 e^{(a_1 + j\omega_1)t'} \;+\; C_2 e^{(a_1 - j\omega_1)t'}$$

$$+\; C_3 e^{(a_2 + j\omega_2)t'} \;+\; C_4 e^{(a_2 - j\omega_2)t'} \qquad\qquad (34)$$

in which the coefficients of the dimensionless time t' are the roots of the characteristic equation

$$\gamma^4 \;+\; A_3\gamma^3 \;+\; A_2\gamma^2 \;+\; A_1\gamma^1 \;+\; A_0 \;=\; 0 \qquad\qquad (35)$$

the A terms being the dimensionless coefficients of Eq. (33). If

AFTR 6590   33

these coefficients are computed for the particular case of <u>neutral stability</u> (by selecting values of R from the graph of Fig. 7) then Eq. 34 must exhibit a sustained (constant amplitude) oscillation. If the frequency of this oscillation is assigned the subscript 1, a_1 must be zero and the coefficients of *(35)* become:

$$A_3 = -2a_2$$

$$A_2 = (a_2^2 + \omega_2^2 + \omega_1^2)$$

$$A_1 = -2a_2\omega_1^2$$

$$A_0 = \omega_1^2(a_2^2 + \omega_2^2)$$

Hence, the roots of *(35)* are readily found:

$$a_2 = -A_3/2$$

$$\omega_1^2 = \frac{A_1}{A_3} = \frac{1}{1 + 1/S(1 + QR)}$$

$$\omega_2^2 = \frac{A_0 A_3}{A_1} - \frac{A_3^2}{4}$$

It will be useful at this point to prepare a graph showing the relation between the frequency of the neutrally damped shimmy and the lateral elasticity K_1. This has been done using Fig. 7b, $(Q = 2)$. Since $T^2/S = K_1 I_w/NK_t$ the values of K_1 may be found by assigning a fixed value to I_w/K_t and to N. Then, (using K_v for the variable K_1)
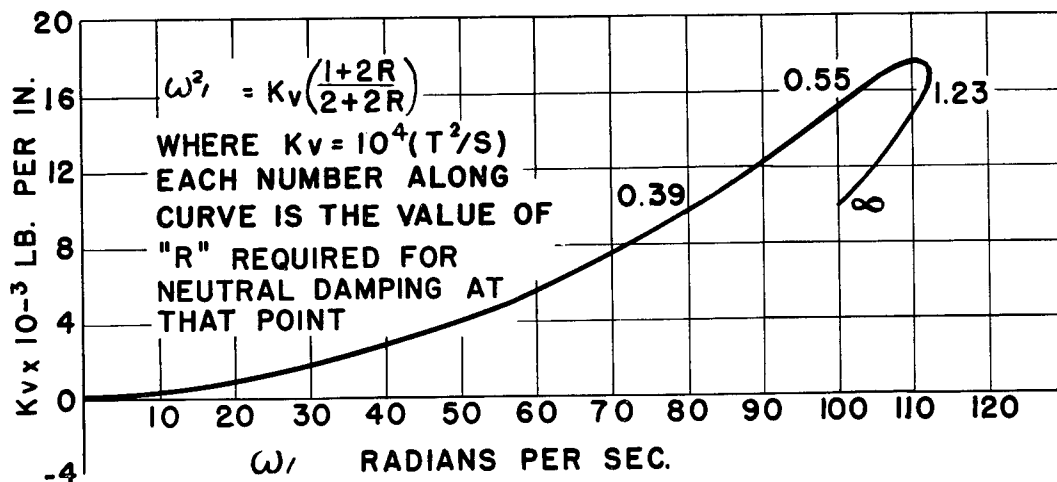
$$K_v = \frac{T^2/S}{I_w/NK_t}$$

and

$$\omega_1^2 = \frac{1}{1 + 1/S(1 + QR)} \times \frac{K_v}{N} \qquad (36)$$

(Where ω_1 is the dimensional shimmy frequency)

Fig. 10 shows the relationship between ω_1 and K_v. The numbers on the graph are the damping ratios required for neutral stability and the ω's are the neutrally damped (N.D.) frequencies.

$$\omega^2{}_1 = K_v\left(\frac{1+2R}{2+2R}\right)$$

WHERE $K_v = 10^4(T^2/S)$
EACH NUMBER ALONG CURVE IS THE VALUE OF "R" REQUIRED FOR NEUTRAL DAMPING AT THAT POINT

NOSEGEAR ELASTICITY vs FREQUENCY

FIGURE 10

Accompanying the motion of frequency ω_1 there is, of course, the motion of frequency ω_2. The latter is usually lower than the former

and is heavily damped. The respective amplitudes of the two frequenc-
ies depend on the initial conditions and the respective modes may
be found from Eq. 34. For example, if in this equation C_3 and C_4 are
made equal to zero, all the initial conditions required from the mode
corresponding to the pure harmonic ω_1 may be found by successive
differentiation of *(34)*. Again, to determine the initial configuration
to insure the presence of the ω_2 motion alone, C_1 and C_2 are set equal
to zero and the above process repeated.

IV. THE INFLUENCE OF THE AIRFRAME

In each of the preceding systems it was assumed that the point
of attachment of the elastic element (K_1) to the airframe remains
fixed laterally - or, more precisely, that the airframe has infinite
mass. But, in order to understand the true nature of the self-excited
vibration and its possible multiple modes of motion, the airframe in-
ertia and elasticity must be considered. The direct method of accom-
plishing this would be to set up the dynamics equations for the over-
all system and obtain the single high-order differential equation
from which the stability criterion and frequencies may be found as
shown in Appendix A. It is, however, simpler and more instructive to
adopt the following procedure.

The method to be described may be considered to be a modification
of the impedance method which makes it applicable to the peculiar
requirements of self-excited vibrations. The procedure is general
and will apply to any linear physical system. The advantages of this
approach are more marked in the case of systems of sixth and higher
order. It is not necessary to solve the high-order differential equat-

ion since the method presents more information about the shimmy and the factors that influence it in a simpler way; but, more important, it permits the use of experimentally determined data in the analysis in such a manner that the effects of controllable parameters can be readily seen. In effect, the system to be analysed has been divided into two fourth-order systems, one of which is self-excited and the other passive. The solutions are obtained by matching the impedances of the two systems at their common junction.

The point of attachment of the elastic element (K_1), the oleo, to the finite mass airframe experiences a lateral displacement (perpendicular to the line of flight) which will be called x_1. If the airplane is rigid all points will turn about a vertical axis which intersects a line along the axles of the main wheels midway between these wheels. Let the moment of inertia of the airplane about this axis be I_0. The natural frequency of the system when the lower end of the oleo is held fixed is $\sqrt{K_1 d^2/I_0}$, where d is the distance from the axis to the strut. The quantity I_0/d^2 may then be used to define an equivalent mass M_1 (i.e. $M_1 = I_0/d^2$) in the equivalent rectilinear system as shown in Fig. 11.

NOTE:

The system illustrated in Fig. 11, though highly idealized, may be used to clarify the significant effects obtained with an actual aircraft. Ground shake tests of a typical airplane were run to determine the modes of motion. A harmonic sidewise force of gradually increasing frequency was applied to the strut at the level of the axle. Resulting motion of the aircraft was recorded with accelerometers. The test arrangement is shown in Fig. 12. Preliminary results show that the node position in the strut moves upward from a point below the ground, passes through the

point at which the vibrator is attached (theoretically infinite coefficient of elasticity) and on up into the fuselage. The node then takes up various positions axially along the fuselage influenced particularly by the phase relation of the wings and stabilizer. It is this point that clearly illustrates the impossibility of defining the lateral elasticity in terms of static measurements. It is a dynamic measurement that may in theory vary from minus infinity to positive infinity.
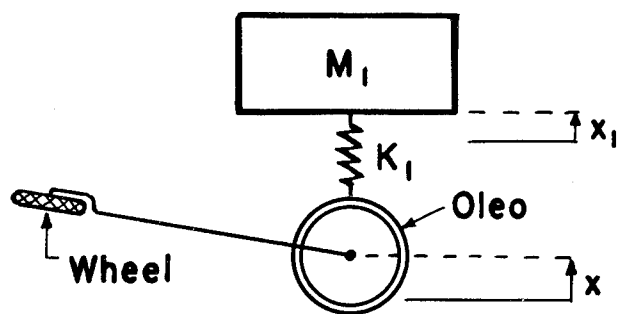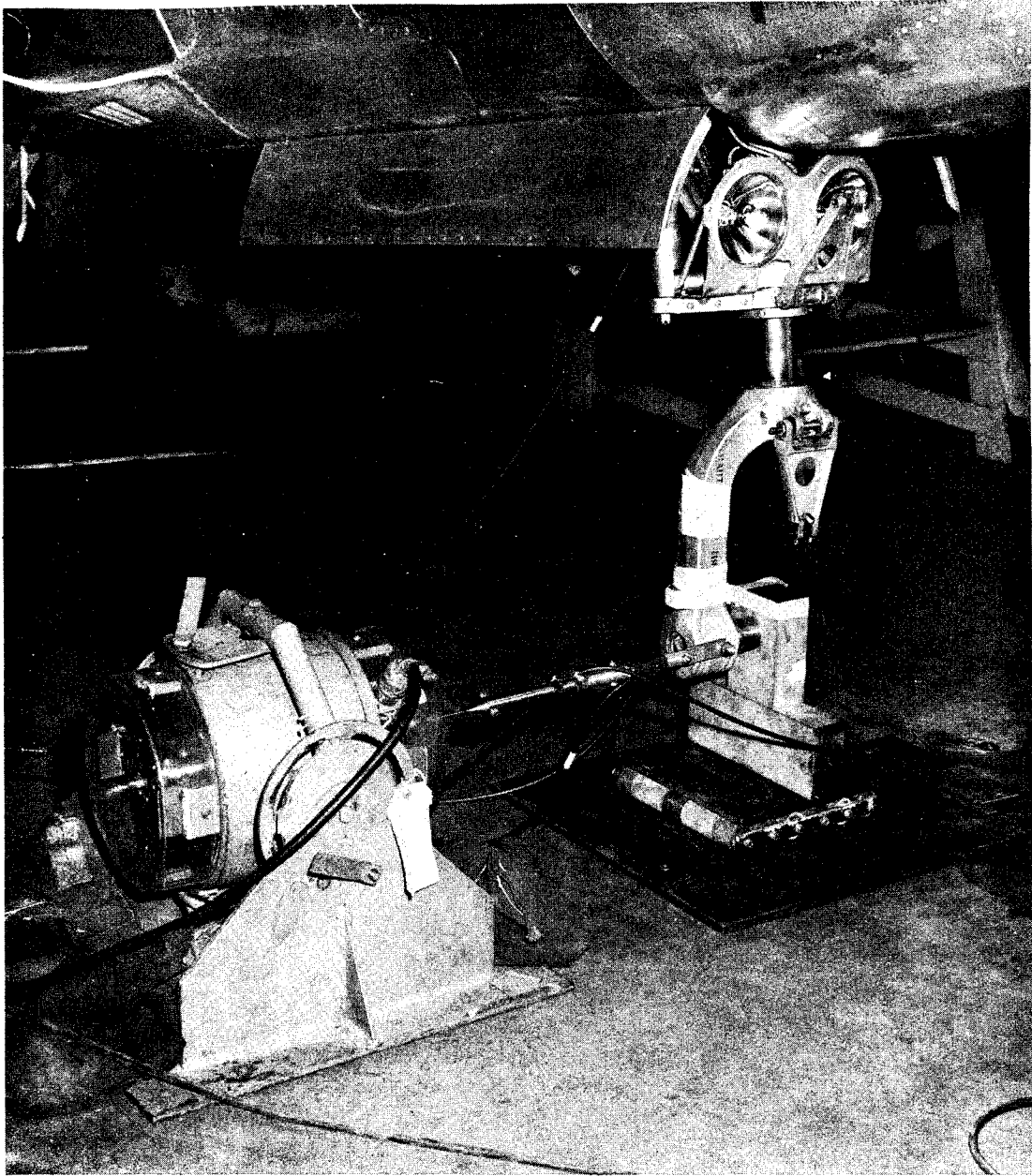

SINGLE MODE AIRFRAME
FIGURE II

In this equivalent system if the lower part of the strut experiences a simple harmonic motion of amplitude $\bar{x}$ and frequency ω it follows that

$$Spring \ force = K_1 \left(\bar{x} \ sin \ \omega t - x_1 \right) = M_1 \ddot{x}_1$$

The particular solution of the above equation is

Ground Shake Test Equipment Arrangement

FIGURE 12

$$x_1 = \frac{K_1/M_1}{(K_1/M_1) - \omega^2} \, \bar{x} \, \sin \omega t$$

$$\text{spring force} = K_1 \bar{x} \sin \omega t \left(1 - \frac{K_1/M_1}{(K_1/M_1) - \omega^2} \right)$$
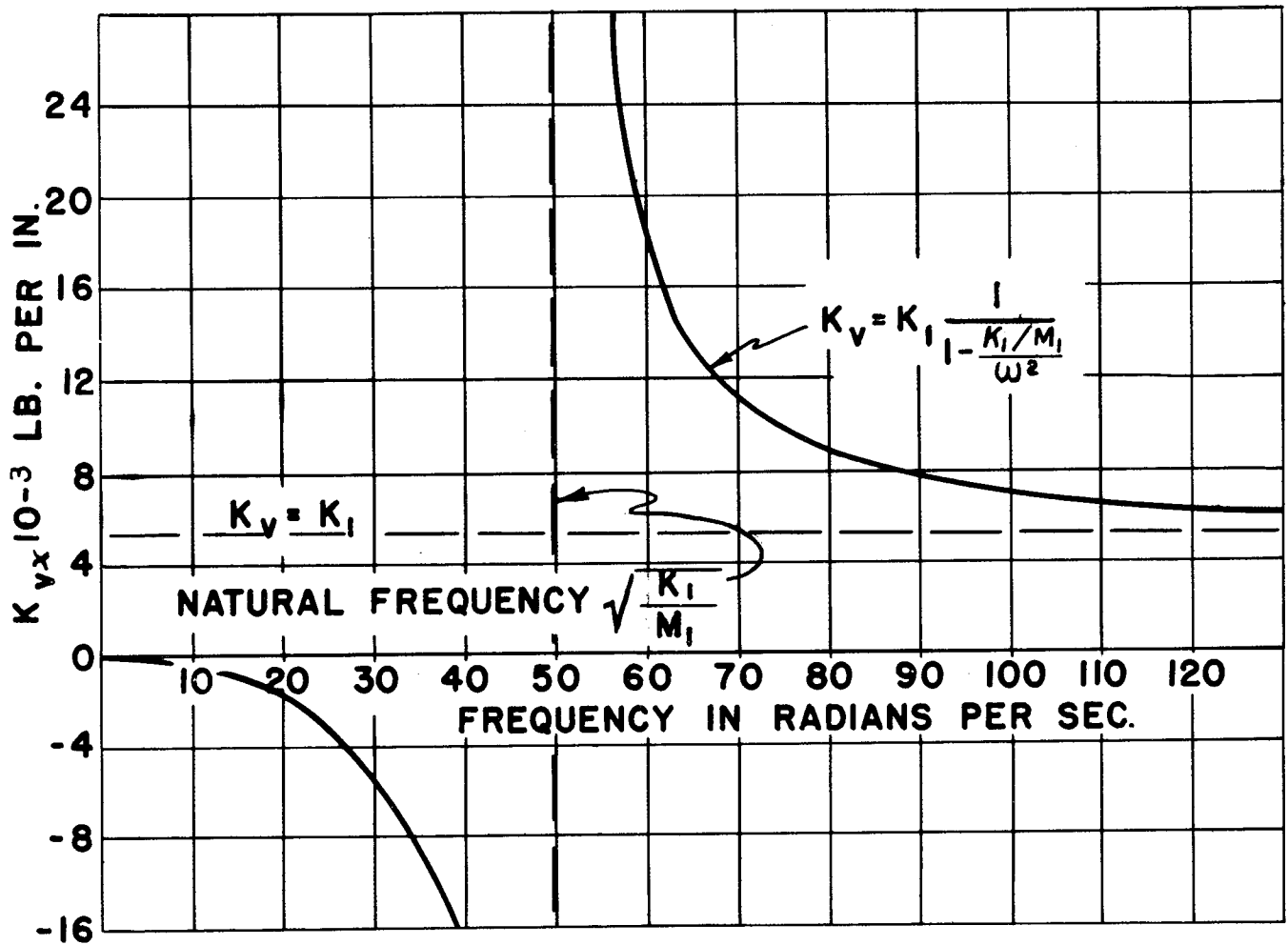
If now the <u>virtual elasticity</u> K_v of the spring is defined as:

$$K_v = \frac{\text{Spring force}}{\bar{x} \, \sin \omega t} = K_1 \, \frac{1}{1 - \frac{K_1/M_1}{\omega^2}} \tag{37}$$

it follows that the elasticity felt by the harmonically vibrating oleo is K_v, a function of frequency as shown in Fig. 13. For example, if the system is vibrating at a frequency less than $\sqrt{K_1/M_1}$ the value of the virtual elasticity K_v as read from the graph is negative. This would make the last term in Eq. 30 negative and hence the system would be statically unstable regardless of the magnitude of the remaining parameters. If the system vibrates with a frequency greater than $\sqrt{K_1/M_1}$ the elasticity felt by the strut is greater than K_1 and, as shown in Graph 7a or 7b, an increase in elasticity (which is proportional to T^2/S) increases the damping required for neutral stability. The effect, then, of the finite mass of the supporting structure is always <u>to reduce stability</u>.

It remains to determine the actual frequency at which the shimmy takes place. Eq. 36 gives the relationship between the frequency and elasticity that exists for the fourth order system when it is neutrally damped. Substituting a series of values of K_1 (which will be called K_v) in this equation will give the sustained harmonic frequency

$$\omega^2 = \frac{1}{1 + 1/S(1 + QR)} \times \frac{K_v}{N} \tag{36}$$

The plot shows a graph with the y-axis labeled "$K_v \times 10^{-3}$ LB. PER IN." ranging from -16 to 24, and the x-axis labeled "FREQUENCY IN RADIANS PER SEC." ranging from 10 to 120.

Labels on the graph:
$$K_v = K_1 \frac{1}{1 - \frac{K_1/M_1}{\omega^2}}$$

$$K_v = K_1$$

NATURAL FREQUENCY $\sqrt{\dfrac{K_1}{M_1}}$

VIRTUAL AIRFRAME ELASTICITY vs. FREQUENCY

FIGURE 13

If now a plot is made of K_v versus ω from Eq. 36 and superimposed on Fig. 13, the point of intersection (A, Fig. 14a) is a point of equilibrium at which the elasticity required to maintain the sustained
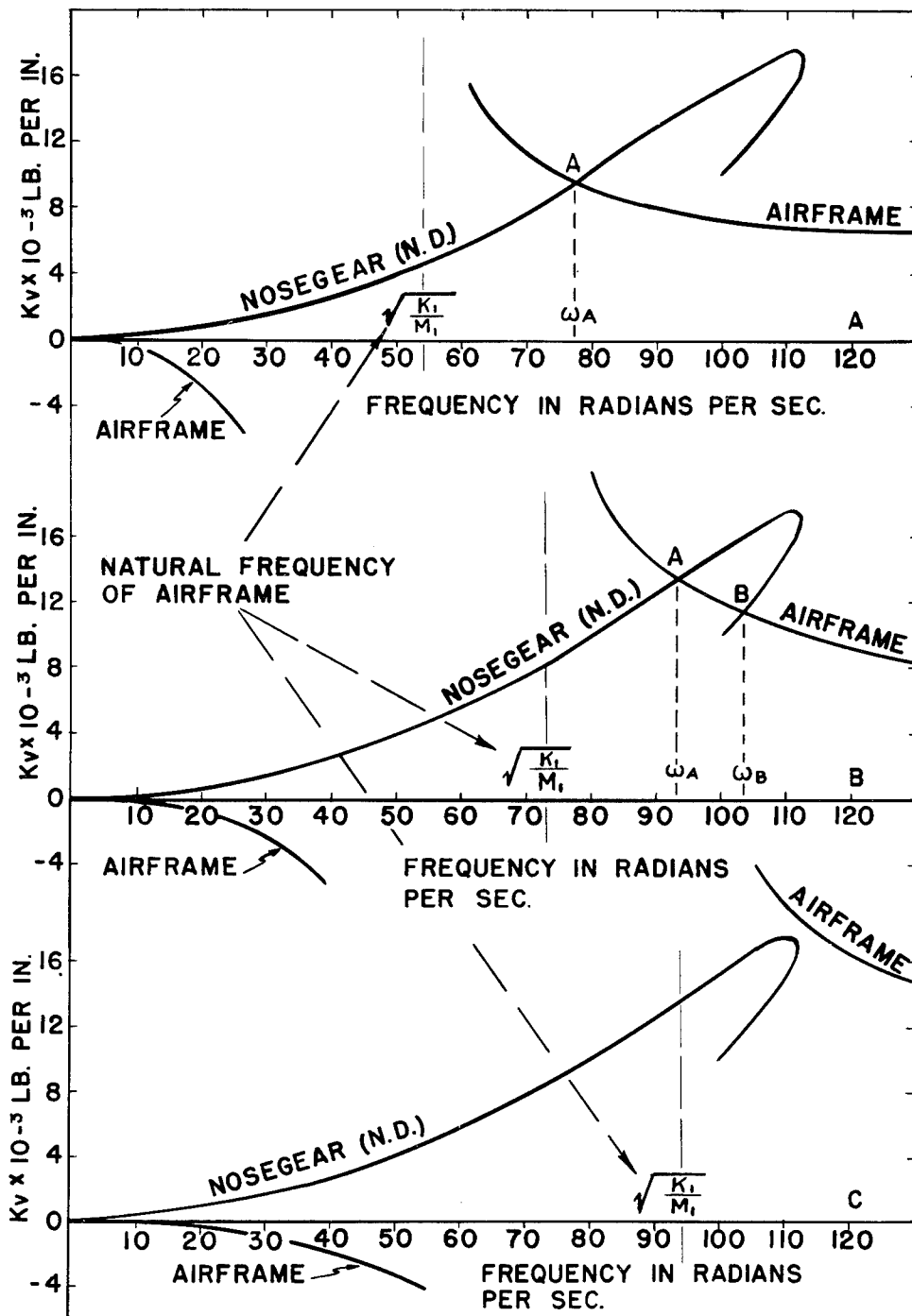
EFFECT OF AIRFRAME ELASTICITY ON NOSEGEAR STABILITY

FIGURE 14

frequency ω is supplied by the virtual elasticity of the given spring K_1. The frequency shown at the point of intersection is the frequency of the neutrally stable shimmy, and the damping ratio shown at the same point is the damping required for neutral stability. Any value of R in excess of this value represents stable motion while any lesser value causes the system to be unstable.

From Fig. 14a it can be seen that the virtual elasticity can never be negative. Also, as M_1 is increased without limit the virtual elasticity approaches K_1 (see Eq. 37). The statement has been made that "when the frequency of the shimmy matches that of some mode of the aircraft violent resonant oscillations will occur." The theory of shimmy as outlined here indicates that there cannot be an accidental coincidence of the shimmy and airframe frequencies. For example, combining Eqs. 36 and 37 gives:

$$\omega^2 = \frac{K_1}{M_1} + \frac{K_1/N}{1 + 1/S(1 + QR)} \qquad (38)$$

Hence, the shimmy frequency always exceeds $\sqrt{K_1/M_1}$, the natural frequency of the single-mass mode.

Rotta (Deutsche Luftfahrtforschung, #8006 p 58, or ATI 26981) states that the torsional rigidity of the aircraft should be large in order not to favor the conditions for shimmy by additional degrees of freedom. But, increasing the rigidity against a particular mode of motion may not influence stability, or it may actually decrease stability, but in no circumstance can it increase stability. For example, Eqs. 8 and 9 show that the lateral elasticity K_1 may be increased without limit and not affect the stability.

Maier suggests (Technische Berichte, #10, 1943) airframe elastic-

ity is a significant factor in shimmy if the natural frequency of the strut and wheel coincides with that of the shimmy. But, in the analysis given above, the reverse of this is seen to be more nearly true, since for large values of $\sqrt{K_1/M_1}$, Eq. 38, the two frequencies referred to by Maier become more widely separated and the system becomes _less_ stable.

If the equivalent mass M_1 of the airframe is gradually reduced, the point of intersection in Fig. 14 gradually moves outward indicating an increase in both the damping required for neutral stability and the shimmy frequency. With M_1 sufficiently reduced the second branch of the virtual elasticity curve will intersect the nose gear curve in two points A and B as shown in Fig. 14b. For this case stability exists for values of the damping ratio R between those shown at A and B. Outside of this range the system is unstable on either side. The sustained frequency for the conditions of point A is ω_A, and, as the damping ratio increases toward B, the stable frequency is interpolated between ω_A and ω_B. (There is, in general, another frequency associated with the one discussed above since this is a fourth order system; this latter is usually relatively small and strongly stable, and its amplitude is determined by the initial conditions. The setting of the torsion spring K_t, i.e. whether it is initally in tension or compression, is one of these conditions). Finally, if the equivalent mass M_1 is still further reduced until the virtual elasticity curve fails to intersect the nose gear curve (Fig. 14c) stability is impossible regardless of the damping employed. This condition could exist in a low-inertia aircraft in combination with a high lateral strut elasticity.
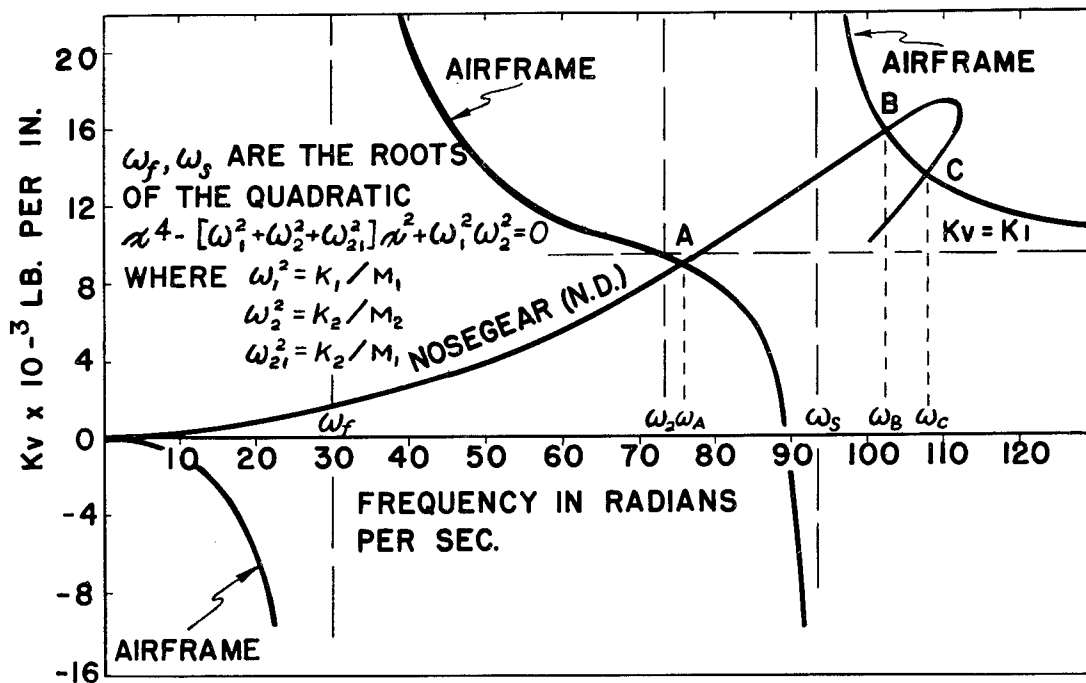
Application to Multiple-Mode Systems:

The method outlined above is general in that it may be applied to the case of airframes that exhibit multiple modes of vibration provided that the virtual elasticity curve is determined experimentally or computed for an equivalent lumped parameter system. For example, if the system can be represented as shown in Fig. 15, and point P is moved with simple harmonic motion of frequency ω, the reaction of the spring K_1 on the oleo at point P can be shown to be that of a simple spring of elasticity (See Appendix C)

$$K_v = K_1 \left[1 - \frac{1 - \omega^2/\omega_2^2}{(1 - \omega^2/\omega_f^2)(1 - \omega^2/\omega_s^2)} \right] \tag{39}$$
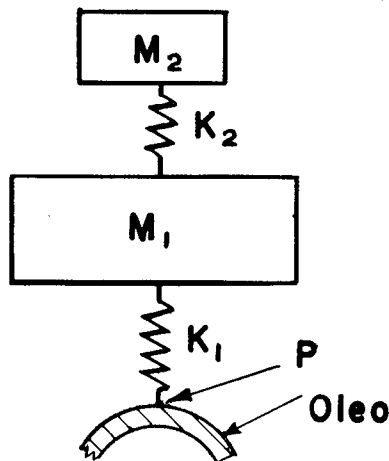
MULTIPLE - MODE AIRFRAME
FIGURE 15

In Eq. 39 K_1 is the static elasticity of the oleo structure, ω_2^2 is K_2/M_2, ω_f is the first natural frequency of the airframe and oleo, while ω_s is the second natural frequency of the same structure. If a plot of K_v versus ω from Eq. 39 is now prepared and superimposed on Fig. 10, the points of intersection will show the frequency and damping ratio required for dynamic <u>equilibrium</u> in the combined system. For example, if the damping ratio is adjusted to the value shown at point A Fig. 16, the system would be in dynamic equilibrium at frequency ω_A. This must be so since if the nose gear were supplied with a fixed-ended spring of elasticity K_A and the damping adjusted to R_A the system would approach a pure harmonic motion of frequency ω_A as time goes on. On the other hand, if the K_1 M_1 K_2 M_2 system is driven at point P with a forced oscillation of frequency ω_A it would react on P as though the spring K_1 were fixed-ended and of elasticity K_v. (This assumes that the initial conditions are chosen so as to eliminate the transient.) Hence, with damping adjusted to R_A, pure harmonic motion would insure a continuous equilibrium of forces throughout the entire cycle. The above argument may be repeated for points B and C. The conclusion to be drawn from this physical analysis of the system is that the general solution of the sixth order differential equation must be so constituted as to be able to provide a solution in pure harmonic motion when the damping ratio is adjusted to any of the three values A, B or C Fig. 16. Point A represents a <u>possible</u> state of motion but one which cannot be realized in any actual case. Only between points B and C can the system be stable. This conclusion is quite general and can be demonstrated by a simple analysis of the sixth order differential equation which represents the system. Let the characteristic equation for this sixth order

The graph shows:

20, 16, 12, 8, 4, 0 (with label $K_V \times 10^{-3}$ LB. PER IN.)

AIRFRAME (upper left), AIRFRAME (upper right with B, C)

ω_f, ω_s ARE THE ROOTS
OF THE QUADRATIC
$\alpha^4 - [\omega_1^2 + \omega_2^2 + \omega_{21}^2]\alpha^2 + \omega_1^2 \omega_2^2 = 0$
WHERE $\omega_1^2 = K_1 / M_1$
$\omega_2^2 = K_2 / M_2$
$\omega_{21}^2 = K_2 / M_1$

NOSEGEAR (N.D.)

$K_V = K_1$

A

B

C

ω_f $\omega_2 \omega_A$ ω_s ω_B ω_c

10 20 30 40 50 60 70 80 90 100 110 120

FREQUENCY IN RADIANS
PER SEC.

-4, -8, -16

AIRFRAME (lower left)

EFFECT OF AIRFRAME ELASTICITY ON NOSEGEAR STABILITY
FOR MULTIPLE - MODE SYSTEM

FIGURE 16

system be (See Appendix A for the differential equation)

$$Y^6 + A_5 Y^5 + A_4 Y^4 + A_3 Y^3 + A_2 Y^2 + A_1 Y + A_0 = 0 \qquad (40)$$

Now consider point A, Fig. 16. With the damping ratio R adjusted to the value corresponding to this point a pure harmonic motion is possible. Hence, under these conditions Eq. 40 must contain a pair of pure imaginary roots, say $\pm j\omega_1$. Dividing (40) by the factor

($\gamma^2 + \omega_1^2$) yields a fourth order equation from which the roots $a_2 \pm j\omega_2$, and $a_3 \pm j\omega_3$ may be found. Repeating this process for points B and C, data is obtained for constructing the graphs of Fig. 17 which is a plot of the real and imaginary root components of Eq. 40 as a function of the damping ratio required for neutral stability.
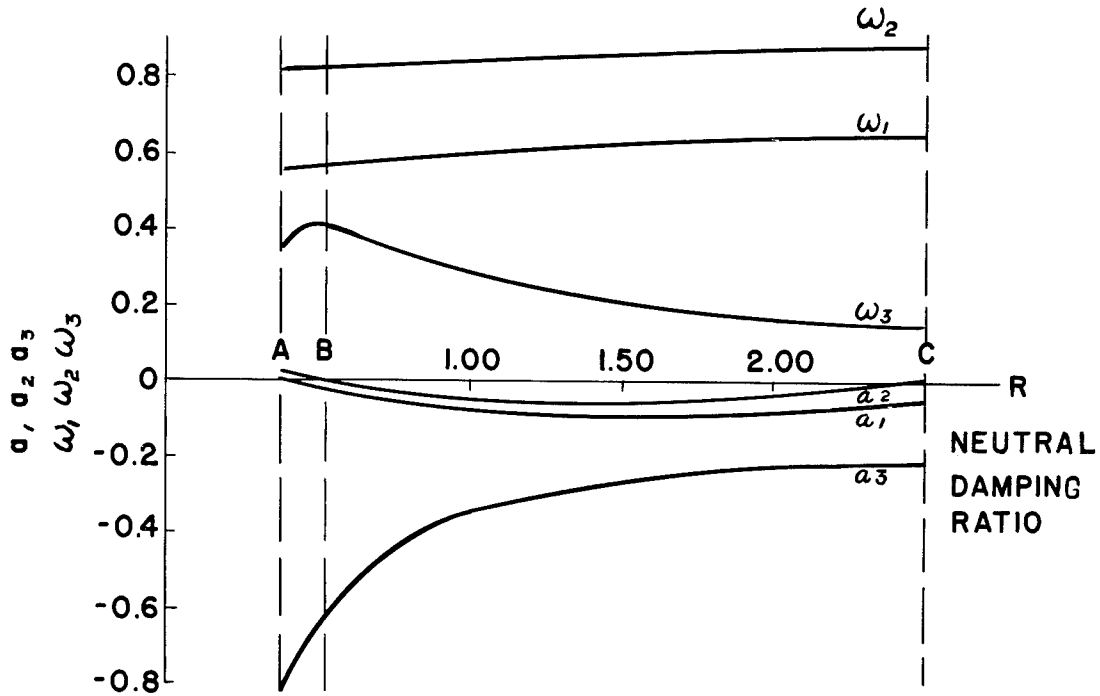
REAL AND IMAGINARY ROOT COMPONETS OF 6th
ORDER EQUATION vs. "R"

FIGURE 17

The general solution for the shimmy amplitude is

$$\theta = C_1 e^{(a_1 + j\omega_1)t'} + C_2 e^{(a_1 - j\omega_1)t'} + C_3 e^{(a_2 + j\omega_2)t'}$$

$$+ C_4 e^{(a_2 - j\omega_2)t'} + C_5 e^{(a_3 + j\omega_3)t'} + C_6 e^{(a_3 - j\omega_3)t'} \tag{41}$$

With R equal to R_A, a_1 is zero and, hence, the sustained frequency is ω_1. For R equal to R_B or R_C, a_2 is zero and, hence, the sustained frequency at these points is ω_2. In general, all three frequencies ω_1, ω_2, and ω_3 are superimposed in the shimmy motion. (This compound harmonic motion has been observed and reported by Guruewicz and Kruse (ATI-23097, translation).

Examination of Fig. 17 shows that points B and C are points of neutral stability, since the plot of a_2 passes through zero at B and C, while outside this range the system is unstable since a_2 is here positive. It is now clear why point A represents a <u>possible</u> mode of motion, since this can be brought about by adjusting the initial conditions so that the amplitudes of both the ω_2 and ω_3 modes are each zero. Obviously, any transient disturbance under these circumstances would cause the ω_2 motion to grow without limit and so, in any actual case, damping below that shown at point B would result in unstable motion.

V. THE USE OF THE CHARTS

For the purpose of analyzing a given system the following steps are recommended:

    1 - Obtain the numerical values of L, m, m_1, f, K_t, and I_w.

        Assign a value to the taxi speed V.

2 - Compute Q and S. Plot R versus T^2/S.   (Eq. 32)

3 - Plot K_v versus ω as in Fig. 10.

4 - Plot K_v as a function of ω by ground shake tests or by calculation using lumped parameters.   (Eq. 39)

5 - The plot *(4)* superimposed on (3) will give points of intersection which disclose the frequencies of neutral shimmy, and the minimum and maximum values of the damping ratio required for stability.

In order to examine the effect of changing the magnitude of any of the system dimensions Fig. 7 should be used. In constructing Fig. 7 eight independent physical parameters are involved, but all the essential information is contained in the three dimensionless numbers Q, S and T^2/S. For example, suppose in a given design

$$Q = 4$$

$$S = 1$$

$$T^2/S = 1$$

Fig. 7b is applicable and from it is found the minimum damping ratio for stability

$$R = 0.64$$

The actual damping is

$$C_t = RC_c = 0.64 \times 2 \sqrt{K_t I_w} \ .$$

Suppose, now, the following modifications are made in the nose-gear design:

Reduce I_w to 1/2 its original value.

Reduce K_t to 3/4 its original value.

" K_1 " 1/2 " " "

These modifications give the following values for the dimensionless parameters:

$$Q = 3.24$$

$$S = 2.0$$

$$T^2/S = 0.33$$

The chart of Fig. 7b may be entered by interpolation with $T^2/S = 0.33$ and $Q = 3.24$ to find $R = 0.42$. The effect of increasing S from 1.0 to 2.0 is slight in this area and may be estimated from Fig. 7a as about 4%. Hence, the modification of the parameters makes the new R about 0.44. Therefore, the new absolute damping (which is proportional to the square root of $K_t \times I_w$) becomes

$$C_t = 0.44 \times 2 \sqrt{(0.75K_t) \times (0.5I_w)}$$

$$\text{or,} \quad C_t = 0.27 \times 2 \sqrt{K_t I_w}$$

Comparing this value of the damping with that originally required shows a reduction of 58%. In addition, it is apparent from Fig. 7b that the parameter changes have removed the operating point from the region in which the upper damping is limited to one in which there is no upper limit. Finally, it can be seen that for any stabilizing damping ratio, say $R = 1.0$, at $T^2/S = 0.33$ the rate of damping of any given initial displacement will be greater than that found at higher values of the inertia ratio, T^2/S. These conclusions may be verified by an inspection of Fig. 7a where it can be seen that the margin of

damping above that required for neutral stability becomes less as T^2/S increases. This of course is due to the upward slope of the neutral stability graphs. (These conclusions have also been verified by studies on an analog computer).

Finally, the effect of varying the trail length L should be examined. It is most significant to note that the inertia ratio, T^2/S, is independent of L. However Q, S and T are functions of L. From the data of the modified structure discussed in the preceeding example, T^2/S = 0.33 and S = 2.0 it follows that T^2 = 0.66 and T = 0.815. Entering Fig. 9a with this value of T it is evident that a given increase in trail will result in a decrease in neutral damping ratio. Considerations other than stability will dictate an upper limit to the trail ratio selected in any given design.

VI. GENERAL NOTES

1 - Vertical Load.

The vertical load on the nose-wheel does not appear directly in the theory presented here. Nevertheless, it is well established that reducing the weight on the nose-wheel does reduce the magnitude of the shimmy. This apparent contradiction is due to the following effects: a) It is tacitly assumed that sufficient weight acts at all times to support the friction force that acts normal to the wheel plane. If the wheel load is reduced and skidding occurs, the energy fed to the system is thereby reduced (See Eq. 20); b) Not only does skidding reduce the energy fed to the system, but, at the same time, it removes energy from the system at the contact point between the wheel and ground, and thus reduces the damper load; c) The lighter

load being accompanied by an extended oleo results in a reduction in the lateral elasticity and thereby increases the inherent stability. (See Fig. 7).

2 - Lateral Elasticity.

The stability criteria established for all but the third-order system show that the damping required for stability is reduced as the lateral elasticity K_1 is reduced. On the other hand, it can be demonstrated that for neutrally damped systems with a given initial disturbance the amplitude of the neutral shimmy is reduced for larger values of the lateral elasticity. (See Eq. 42). These two statements are not contradictory but do require careful judgement in their appliation. For example, accompanying the reduced amplitude in the latter case, there will be increased frequency, spindle acceleration, and force transmitted to the fuselage. Hence, it may be unwise to attempt to fight a shimmy by opposing it directly with increased lateral rigidity. In this connection, it is planned to investigate the possibilities of shock mounting the nose-gear to reduce the lateral elasticity over a limited range of amplitude. This, of course, makes the system nonlinear, and may best be handled by an analog computer.

3 - High-Frequency Modes of Motion.

From Fig. 16 it appears that if the airframe contains modes of motion with sufficiently high frequencies, no amount of damping can theoretically stabilize the system. Actually, the high frequency intersections imply correspondingly high virtual lateral elasticity so that if a pure high frequency mode is initially set up, its am - plitude is relatively small and is effectively checked by inherent

hysteresis damping. In addition, it is expected that for the more likely initial disturbances, the conditions for exciting the lower mode will be more favorable.

4 - Velocity Effects.

The amplitude (Eq. 42), frequency (Eq. 38), and damping required (Fig. 8) of a neutrally stable mode increase only, slightly with taxi velocity. However, strut acceleration, spindle force and ground force normal to the wheel plane increase approximately in direct proportion to that velocity. This information may be found from the solution of Eq. 8 for an initial condition of θ_0:

$$\frac{\theta}{\theta_0} = \frac{1}{\sqrt{1 + L^4 K_1 / V^2 I_w}} \ cos(\omega t + \varphi) \qquad (42)$$

Experimental evidence usually supports the view that the severity of shimmy actually grows less with increased taxi speed. This is completely false security since the observed diminution of shimmy meant simply that other conditions (e.g. sufficient tire friction force) were unfavorable to maintaining the vibration. Guroewicz and Kruse, (Untersuchung Des Spornflatterns FW190, ATI-23097) discuss a case in which shimmy appeared to rise and fall between 80 km per hour and 90 km per hour. This phenomenon may be mistaken for simple resonance, but when other factors are correct the shimmy may return in full violence at higher speeds as was actually observed in these tests.

5 - Stability Without Damping.

Stability can be obtained without damping. For example, if the damper piston is locked in position the swivel torque (Eq. 25, p 16)

becomes

$$F_n a - F_l b - K_t \theta = I_g \ddot{\theta}$$

Combining this with Eq. 23 through Eq. 28 gives

$$(I_g + m_1 L^2 + ma^2) \dddot{\theta} + V(m_1 L + ma) \ddot{\theta} + (K_t + K_1 L^2) \dot{\theta} + K_1 LV\theta = 0$$

(Compare with Eq. 30). Applying Routh's criterion to the above equation, the condition for stability with a locked damper is

$$K_t > K_1 I_w / N$$

6 - **Shimmy Frequencies For Neutrally Damped Systems**.

a) **Third order system:**

$$\omega^2_{Shimmy} = K_1 L^2 / I_w + NL^2 \qquad (\text{From Eq. 8 })$$

b) **Fourth order system:**

$$\omega^2_{Shimmy} = \frac{K_1/N}{1 + 1 / S(1 + QR)} \qquad (\text{Eq. 36})$$

c) **Fourth order system with one degree of freedom in the airframe.**

$$\omega^2_{Shimmy} = K_1/M_1 + \frac{K_1/N}{1 + 1 / S(1 + QR)} \qquad (\text{Eq. 38})$$

d) **Sixth order system. (Two degrees of freedom in the airframe).**

$$\omega^2_{Shimmy} = (\omega_f^2 + \omega_s^2 + Z \pm \sqrt{(\omega_f^2 + \omega_s^2 + Z)^2 - 4[\omega_f^2\omega_s^2 + Z(\omega_f^2 + \omega_s^2 - \omega_1^2)]})1/2$$
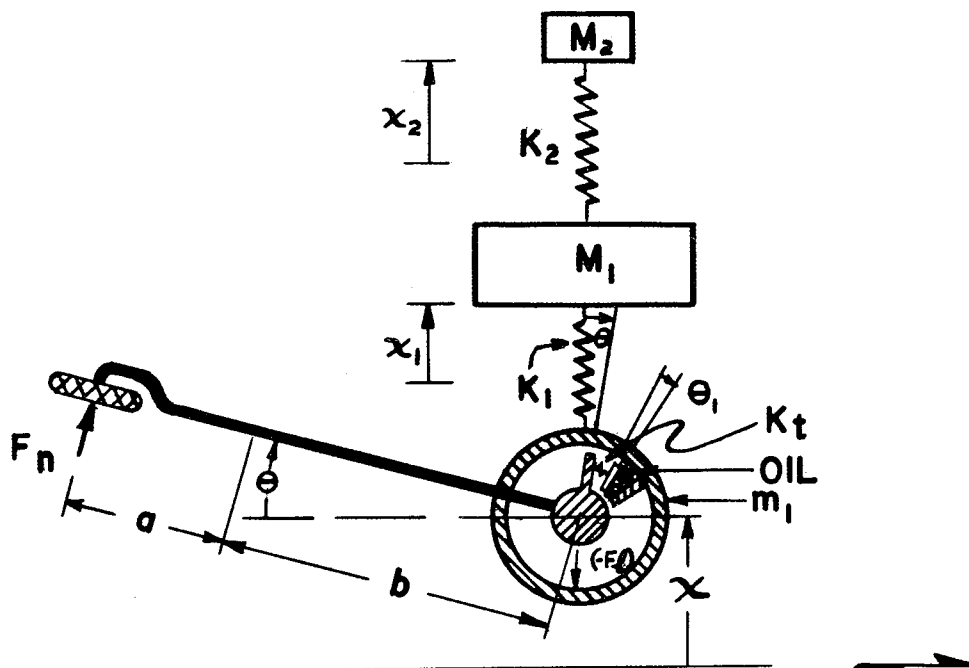
Where

$$Z = \frac{K_1/N}{1 + 1/S(1 + QR)} \qquad \text{(From Eqs. 36 and 39)}$$

Use plus sign for all neutrally stable systems. ω_f is the first natural frequency of the system, ω_s the second natural frequency of the system, and $\omega_1 = \sqrt{K_1/M_1}$.

FOURTH ORDER SYSTEM WITH MULTIPLE-MODE AIRFRAME

FIGURE A-1

Differential Equation for the Nose-Wheel Gear with Two Degrees of Freedom in the Air Frame.

The simultaneous differential equations for this case (See Fig. A1) are:

Forces:

$$F_n + F_l = m\ddot{x}_g \tag{A1}$$

$$- F_l - K_1(x - x_1) = m_1\ddot{x} \tag{A2}$$

$$K_2(x_2 - x_1) + K_1(x - x_1) = M_1\ddot{x}_1 \tag{A3}$$

$$- K_2(x_2 - x_1) = M_2\ddot{x}_2 \tag{A4}$$

Swivel Torque:

$$F_n a - F_l b - C_t\dot{\theta}_1 = I_g\ddot{\theta} \tag{A5}$$

Damper Torque:

$$C_t\dot{\theta}_1 = K_1(\theta - \theta_1) \tag{A6}$$

Kinematic:

$$- L\dot{\theta} = \dot{x} + V\theta \tag{A7}$$

Geometric:

$$x_g = x + b\theta \tag{A8}$$

Combining the above equations gives the following differential equation in θ:

$$[C_t(I_w + L^2N)]D^8\theta + [K_t(I_w + L^2N) + C_tVLN]D^7\theta$$

$$+ [K_tVLN + C_t\{K_t + L^2K_1 + (I_w + L^2N)(K_1/M_1 + K_2/M_2 + K_2/M_1)\}]D^6\theta$$

$$+ [K_1(K_tL^2 + C_tVL) + \{K_t(I_w + L^2N) + C_tVLN\}(K_1/M_1 + K_2/M_2 + K_2/M_1)]D^5\theta$$

$$+ [K_1 K_t VL + C_t (K_1/M_1)(K_2/M_2) \left\{ I_w + L^2(N + M_1 + M_2) \right\}$$

$$+ K_t (VLN + C_t)(K_1/M_1 + K_2/M_2 + K_2/M_1)] D^4 \theta$$

$$+ (K_1/M_1)(K_2/M_2)[K_t \left\{ I_w + L^2(N + M_1 + M_2) \right\} + C_t VL(N + M_1 + M_2)] D^3 \theta$$

$$+ (K_t)(K_1/M_1)(K_2/M_2)[VL(N + M_1 + M_2) + C_t] D^2 \theta = 0 \qquad (A9)$$

Substituting the following non-dimensional numbers

$$r_1^2 = \frac{K_1/M_1}{K_1/N}$$

$$r_2^2 = \frac{K_2/M_2}{K_1/N}$$

$$r_{21}^2 = \frac{K_2/M_1}{K_1/N}$$

$(Q, S, T,$ and R as previously defined$)$ gives the following different-
ial equation in θ where the derivative is taken with respect to the
dimensionless time $\sqrt{K_1/N}$ t:

$$D^8 \theta + \frac{(T/2\sqrt{S})[1 + S(1 + QR)]}{(T^2/S)(1 + S)R} D^7 \theta$$

$$+ \frac{[QS/4 + R \left\{ 1 + T^2 + (T^2/S)(1 + S)(r_1^2 + r_2^2 + r_{21}^2) \right\}]}{(T^2/S)(1 + S)R} D^6 \theta$$

$$+ \frac{(T/2\sqrt{S})[S(1 + QR)(1 + r_1^2 + r_2^2 + r_{21}^2) + r_1^2 + r_2^2 + r_{21}^2]}{(T^2/S)(1 + S)R} D^5 \theta$$

$$+ \frac{1}{(T^2/S)(1 + S)R} \left[(QS/4)(1 + r_1^2 + r_2^2 + r_{21}^2) \right.$$

$$+ R\left\{ r_1^2 + r_2^2 + r_{21}^2 + (r_1^2 r_2^2)(T^2/S)(1 + S[1 + 1/r_1^2 + r_{21}^2/r_1^2 r_2^2]) \right\} \right] D^4\theta$$

$$+ \frac{(r_1^2 r_2^2)(T/2 \sqrt{S})[1 + S(1 + QR)(1 + 1/r_1^2 + r_{21}^2/r_1^2 r_2^2)]}{(T^2/S)(1 + S)R} D^3\theta$$

$$+ \frac{(r_1^2 r_2^2)\ (QS/4)(1 + 1/r_1^2 + r_{21}^2/r_1^2 r_2^2) + R]}{(T^2/S)(1 + S)R} D^2\theta = 0 \qquad (A10)$$

By setting $M_1 = \infty$ and $K_2 = 0$ eliminates the effect of the airframe and thus reduces the 6th order equation to 4th order.

$$D^8\theta + \frac{(T/2 \sqrt{S})[1 + S(1 + QR)]}{(T^2/S)(1 + S)R} D^7\theta + \frac{[(1 + T^2)R + QS/4]}{(T^2/S)(1 + S)R} D^6\theta$$

$$+ \frac{(T/2 \sqrt{S})[S(1 + QR)]}{(T^2/S)(1 + S)R} D^5\theta + \frac{QS/4}{(T^2/S)(1 + S)R} D^4\theta = 0 \qquad (A11)$$

TIRE ELASTICITY

The effect of tire elasticity and creep is confined to the kinematic Eq. A7 as shown in the following analysis:
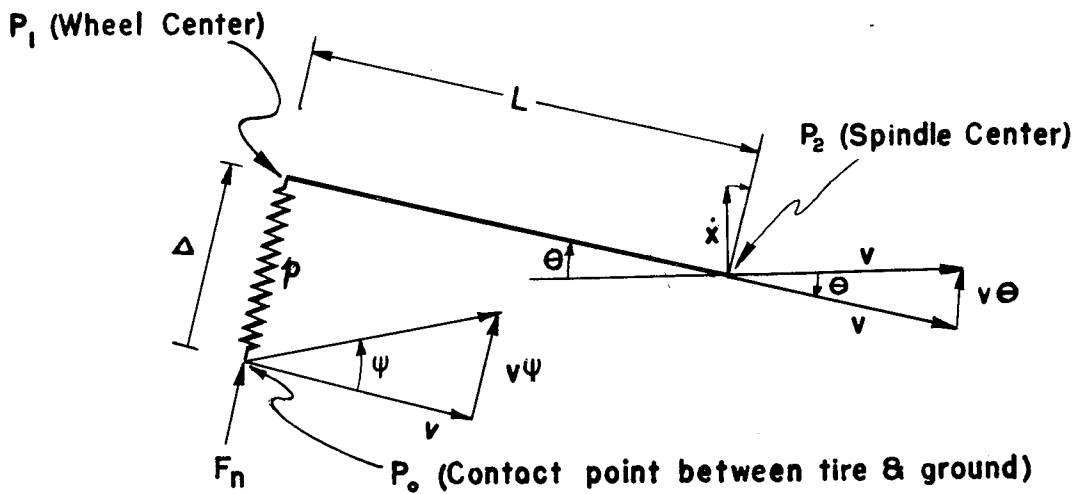

DIAGRAM OF TIRE CHARACTERISTICS

FIGURE   B - 1

The point P_O moves over the ground at an angle to the plane of the wheel due to the force F_n. But since time is required to establish this angle ψ we have:

$$\psi + C_1\dot{\psi} = -CF_n$$

or

$$\psi = \frac{-CF_n}{1 + C_1 D}$$

Where C_1 is the time constant of this assumed first order system. Due to this slip angle ψ, the point P_O has a velocity normal to the wheel plane equal to $V\psi$. But because the tire is elastic, the wheel center P_1 can move relative to P_O. The actual stretch (Δ) between P_O and P_1 is due to the force F_n transmitted from the ground thru the tire. Hence,

$$\Delta = -pF_n \quad \text{Where } p \text{ is the tire compressibility.}$$

$$\dot{\Delta} = -p\dot{F}_n$$

The total normal velocity of P_1 is thus:

$$-\frac{CF_n V}{1 + C_1 D} - p\dot{F}_n$$

And the angular velocity of the link is the velocity of P_1 relative to P_2, or:

$$L\dot{\theta} = \left(-\frac{CF_n V}{1 + C_1 D} - p\dot{F}_n \right) - (\dot{x} + V\theta) \qquad (B1)$$

For the usual range of shimmy frequencies, it can be shown that the effect of time constant C_1 can be represented approximately by replacing Eq. B1 with:

$$L\dot{\theta} = -\frac{1}{40} CF_n V - p\dot{F}_n - (\dot{x} + V\theta) \qquad (B2)$$

Eq. B2 may now replace the kinematic equation in any of the previous systems. For example, when Eq. B2 is combined with those of the fourth order system and non-dimensionalized by substituting

$$M_r = (1 - f)m/N$$

$$U = pK_1$$

$$W = \frac{K_1 CV}{40 \sqrt[4]{K_1/N}}$$

Q, S, T, R, and dimensionless time $\sqrt{K_1/N}\ t$ as before, we have:

$$(UT^2/S)R[M_r + 1 + M_r S]D^6\theta + (T/\sqrt{S})[(M_r + 1 + M_r S)(U/2 + WRT/\sqrt{S})]D^5\theta$$

$$+ [UR\{T^2/S + 1 + M_r(1 + T^2)\} + (WT/2\sqrt{S})(M_r + 1 + M_r S) + (1 + S)RT^2/S]D^4\theta$$

$$+ [(UT/2\sqrt{S})(1 + M_r S) + WR\{T^2/S + 1 + M_r(1 + T^2)\} + (T/2\sqrt{S})(1+S+ SQR)]D^3\theta$$

$$+ [UR + (WT/2\sqrt{S})(1 + M_r S) + (1 + T^2)R + QS/4]D^2\theta$$

$$+ [WR + (T/2\sqrt{S})S(1 + QR)]D\theta + (QS/R)\ \theta = 0 \qquad (B3)$$

Setting p and C equal to zero reduces $(B3)$ to the fourth order:

$$[(T^2/S)(1 + S)R]D^4\theta + (T/2\sqrt{S})[1 + S + SQR]\ D^3\theta + [(1 + T^2)R$$

$$+ QS/4]D^2\theta + (T/2\sqrt{S})[S(1 + QR)]D\theta + [QS/4]\ \theta = 0 \qquad (B4)$$

The above procedure differs from that outlined by Von Schlippe in that no account is taken of the shift of the force center in the

tire footprint. In an actual shimmy, the pattern of tire distortion representing this shift would have to be established and erased approximately 25 times per second. As yet, there is no experimental evidence that this action takes place, or that its influence can be anything but trivial. However, when Eq. B2 was used in place of the previous kinematic equation and the two compared on an analog, the system having the tire constants proved to be more stable. Example of the results are given in Fig. B2.

An experimental program on the mechanical properties of pneumatic tires will be conducted at the Aircraft Laboratory at Wright Field and one of its major objectives will be to explore the part played by the tire in the phenomenon of shimmy.

FIGURE B 2
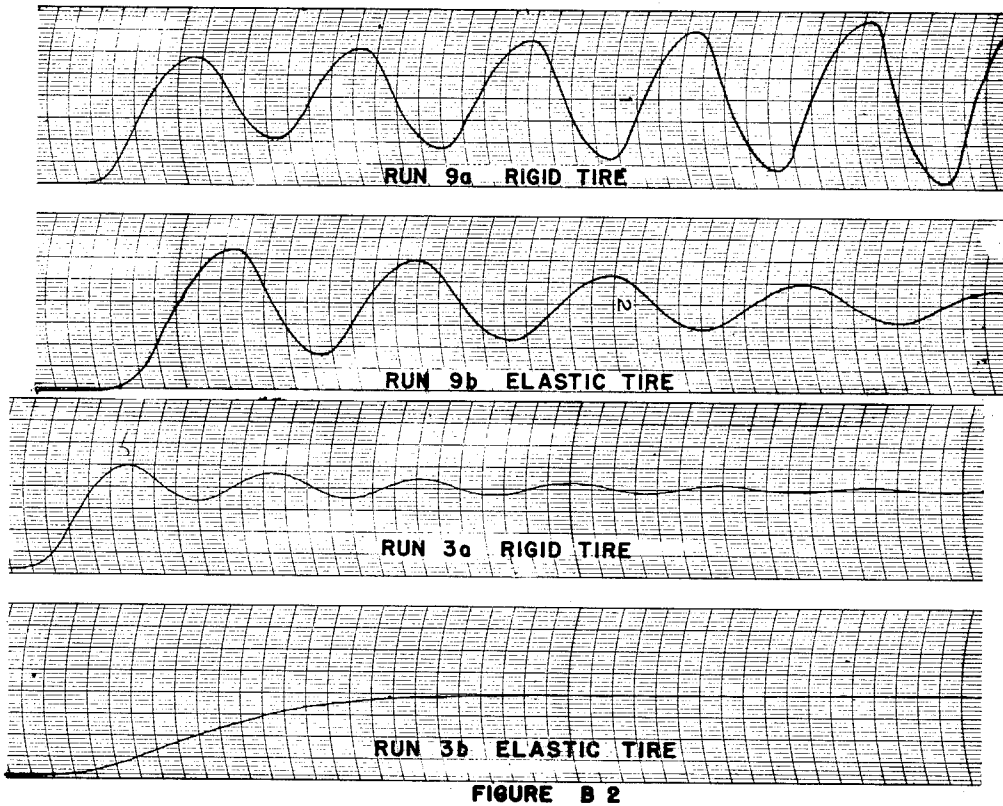
VIRTUAL ELASTICITY

The equivalent lumped paramater system of the airframe is shown in Fig. C1. Point P represents the point of attachment of the equivalent elastic element to the oleo. K_1 represents the combined lateral elasticity of the oleo and the torsional elasticity of the fuselage.
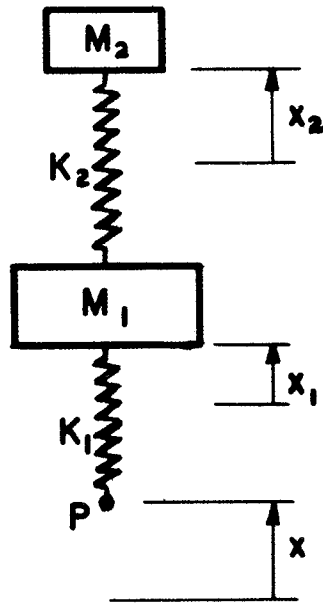
EQUIVALENT AIRFRAME SYSTEM

FIGURE C-I

Considering the forces on M_1:

$$K_1(x - x_1) - K_2(x_1 - x_2) = M_1\ddot{x}_1 \qquad (C1)$$

And for M_2

$$K_2(x_1 - x_2) = M_2\ddot{x}_2 \qquad (C2)$$

Substituting $D^2 x_2$ for $\ddot{x}_2$ in Eq. C2, and solving for x_2 gives

$$x_2 = x_1 \frac{K_2}{K_2 + M_2 D^2} \qquad (C3)$$

(D stands for the differential operator). Substituting Eq. C3 in Eq. C1 gives

$$\ddddot{x}_1 + (K_1/M_1 + K_2/M_2 + K_2/M_1)\ \ddot{x}_1 + (K_1 K_2/M_1 M_2)x_1 =$$

$$(K_1 K_2/M_1 M_2)x + (K_1/M_1)\ \ddot{x} \qquad (C4)$$

If P is assumed to have simple harmonic motio⁻ o⁺ ⸱requency ω and amplitude $\bar{x}$ then,

$$x = \bar{x}\ cos\ \omega t$$

and Eq. C4 becomes

$$\ddddot{x}_1 + (\omega_1^2 + \omega_2^2 + \omega_{21}^2)\ \ddot{x}_1 + \omega_1^2\omega_2^2 x_1 = \omega_1^2\omega_2^2(1 - \omega^2/\omega_2^2)\bar{x}\ cos\omega t \qquad (C5)$$

Whe⸱⸱ $\omega_1^2 = K_1/M_1$, $\omega_2^2 = K_2/M_2$ and $\omega_{21}^2 = K_2/M_1$.

Assume for a trial solution that x_1 is $A\ cos\ \omega t$. Then Eq. C5 becomes

$$[\omega^4 - (\omega_1^2 + \omega_2^2 + \omega_{21}^2)\omega^2 + \omega_1^2\omega_2^2]A cos\ \omega t = \omega_1^2\omega_2^2(1 - \omega^2/\omega_2^2)\bar{x}cos\omega t$$

It can be seen that $A\ cos\ \omega t$ is a steady-state solution of Eq. C5 if

$$A = \frac{\omega_1^2 \omega_2^2 (1 - \omega^2/\omega_2^2)\,\bar{x}}{\omega^4 - (\omega_1^2 + \omega_2^2 + \omega_{21}^2)\,\omega^2 + \omega_1^2 \omega_2^2}$$

The denominator of this expression may be written in terms of its factors as

$$(\omega^2 - \omega_f^2)(\omega^2 - \omega_s^2)$$

Where ω_f is the first natural frequency of the system, (i.e. the value of ω that causes A to become infinite), and ω_s is the second natural frequency. Therefore

$$A = \frac{\omega_1^2 \omega_2^2 (1 - \omega^2/\omega_2^2)\,\bar{x}}{\omega_f^2 \omega_s^2 (1 - \omega^2/\omega_f^2)(1 - \omega^2/\omega_s^2)} \qquad (C6)$$

But $\omega_1^2 \omega_2^2 = \omega_f^2 \omega_s^2$ since the last term of the biquardratic is the product of its roots. The downward force exerted on P at any instant t is $K_1(x - x_1)$, and hence, the **virtual elasticity** K_v against which P acts is

$$K_v = \frac{K_1(x - x_1)}{x} = \frac{K_1(\bar{x} - A)\,\cos \omega t}{\bar{x}\,\cos \omega t}$$

or

$$K_v = K_1 \left[1 - \frac{1 - \omega^2/\omega_2^2}{(1 - \omega^2/\omega_f^2)(1 - \omega^2/\omega_s^2)} \right] \qquad (C7)$$

As shown by the graph of this equation (See Fig. 16) the virtual elasticity is **negative** from $\omega = 0$ to $\omega = \omega_f$. It then becomes infinite and positive until, at $\omega = \omega_2$, the virtual elasticity equals the actual elasticity K_1. Further increase in the forcing frequency causes

K_v to pass through zero and become minus infinity at $\omega = \omega_s$. Beyond this frequency the value of K_v passes from positive infinity and becomes asymptotic to K_1 as the forcing frequency increases without limit.

BIBLIOGRAPHY

Howard, Walter B., Jr. A Full Scale Investigation of the Effect of Several Factors on the Shimmy of Castering Wheels. NACA TN-760.

Temple, G. Large Angle Shimmy. Issue ATI-51760, 1943.

Temple, G. A Simplified General Theory of Wheel Shimmy. Issue ATI-40742, June 1942.

Guroewicz and Kruse. Untersuchung Des Spornflatterns FW. 190. ATI-23097.

Rotta. Deutsche Luftfahrtforschung. #8006 ATI-26981.

Maier. Technische Berichte. #10, 1943.

Dietz, O. and Harling R. Seitensteifigkeit und Seitenfuhrung von Flugzeugrefen. ATI-19805, October 1941.

Dietrich, R., and Schlippe, B. Shimmying of a Pneumatic Wheel. ATI-18920, October 1941.

Dietz, O. and Harling, R. Tail Wheel Flutter. ATI-34467.

Dietrich, R., and Schlippe, B. Flutter of a Wheel With Pneumatic Tire. ATI-51760, October 1943.

Fromm, H. Damping of Wheel Shimmy. ATI-57687, October, 1941.

Maier, E. Theoretical Investigations of the Stability of Landing Gears. German Document 962-2995-1, Jan. 1940.

Kantrowitz, A. Stability of Castering Wheels for Aircraft Landing Gears. NACA Report 686, 1940.

Lauber, J. E. Dynamic Analysis of Nose Wheel Shimmy on the C-124 Airplane. Douglas Aircraft Co. Report No. SM-13814.

Waterman, L. T. Shimmy Characteristics of Dual Landing Gears. Fairchild Engine and Airplane Corporation, Engineering Report No. SR-11.

Riekert, P. Shimmy Vibrations in Landing Gear. 962-1851-1, ATI-57682.

Dietz, O. and Harling, R. Experimental Investigation of Tail-Wheel Shimmy. ATI-68437.

Maier, E., and Renz, M. Shimmy Vibration of Dual Wheels on Tricycle Gear. 962-2241-1, ATI-22381.

Schlippe, B. Shimmying of Wheels Equipped with Pneumatic Tires. ATI-51760.

Schrode H. Reduction of Flutter of Tail and Nose Wheels. ATI-74544.